The Thesis Committee for Shawn Curtis Hutcherson
Certifies that this is the approved version of the following thesis:

Analysis of a Database of Uniaxial Geogrid Pullout Resistance Results

APPROVED BY
SUPERVISING COMMITTEE:

Supervisor:

Jorge G. Zornberg

Robert B. Gilbert

Analysis of a Database of Uniaxial Geogrid Pullout Resistance Results

by

Shawn Curtis Hutcherson, B.S.

Thesis

Presented to the Faculty of the Graduate School of

The University of Texas at Austin

in Partial Fulfillment

of the Requirements

for the Degree of

Master of Science in Engineering

The University of Texas at Austin

August 2012

Acknowledgements

I would like to thank Dr. Jorge Zornberg for encouraging me to pursue the research option. Working with him and the rest of his research team has been an extremely rewarding experience, and has helped to foster a great relationship with all.

I would also like to thank SGI Testing Services, Tensar and CETCO for their support on this project.

Abstract

Analysis of a Database of Uniaxial Geogrid Pullout Resistance Results

Shawn Curtis Hutcherson, MSE

The University of Texas at Austin, 2012

Supervisor: Jorge Zornberg

Being able to extrapolate interaction values from a database of pullout resistance testing results may possibly help with narrowing down the most suitable reinforcement/fill material combinations for a Mechanically Stabilized Earth wall, thereby reducing the number of tests needed for a design and maximizing the efficiency of the system.

The objectives of this thesis include the following: collect and organize a broad collection of data in a way that can assist in preliminary selection of interaction properties for uniaxial geogrids; analyze the collection of data for trends related to geogrid polymer type; analyze the collection of data for trends related to the presence of fines in the fill material; compare the collected data to previous studies on the effects of geogrid specimen length on pullout performance; and compare the collected data to previous studies on the effect of geogrid rib thickness to mean particle size ratio on normalized bearing stress and CI values.

The data from 101 pullout tests are presented in tabular and graphic form so that the coefficient of interaction may be interpolated for many geogrid/fill material combinations. The effect of polymer type (PET vs HDPE) was shown to have little effect on how a geogrid performs in a fill material. In one case, the two polymer types exhibit differing trends within the same fill material. The presence of fines (>12% by weight) in the fill material results in a significant decrease in the coefficient of interaction when compared to clean granular fills. The effects of geogrid embedment length have significant effects on the results of geogrid pullout tests. Samples with shorter lengths were shown to carry a greater load per unit area than longer samples. Normalized bearing stress is shown to be heavily influenced by the geogrid transverse rib thickness to mean particle size ratio (B/D_{50}). For a particular fill material, normalized bearing stress decreases linearly with increasing B/D_{50}. For a particular geogrid, normalized bearing stress is shown to have a bi-linear behavior with increasing B/D_{50}. Initially, normalized bearing stress increases with increasing B/D_{50}. After reaching a peak, normalized bearing stress begins to decrease with increasing B/D_{50}.

Table of Contents

List of Tables

List of Figures

Chapter 1: Introduction

1.1 MOTIVATION OF THIS STUDY

Many civil engineering projects require alterations to be made to the existing ground line. These projects have permitted limits of construction (LOC) that prevent the construction activities from causing physical disturbance to surrounding properties. In order to build a structure of a given size within the LOC, it is at times necessary to steepen soil slopes or construct vertical walls to accommodate the changes in the grade line. In the case of a soil slope, the maximum angle an unrestrained slope can safely tolerate depends on the shear strength of the in-situ soil. A stability analysis will reveal whether or not an adequate factor of safety (FS) against slope failure can be obtained for the proposed slope angle, which can range from zero to 90 degrees, using the in-situ soil without reinforcement. If the stability analysis reports an insufficient FS, the slope will need to be reinforced. Many options are available for reinforcing a soil slope, including Mechanically Stabilized Earth (MSE) walls and Reinforced Soil Slopes (RSS).

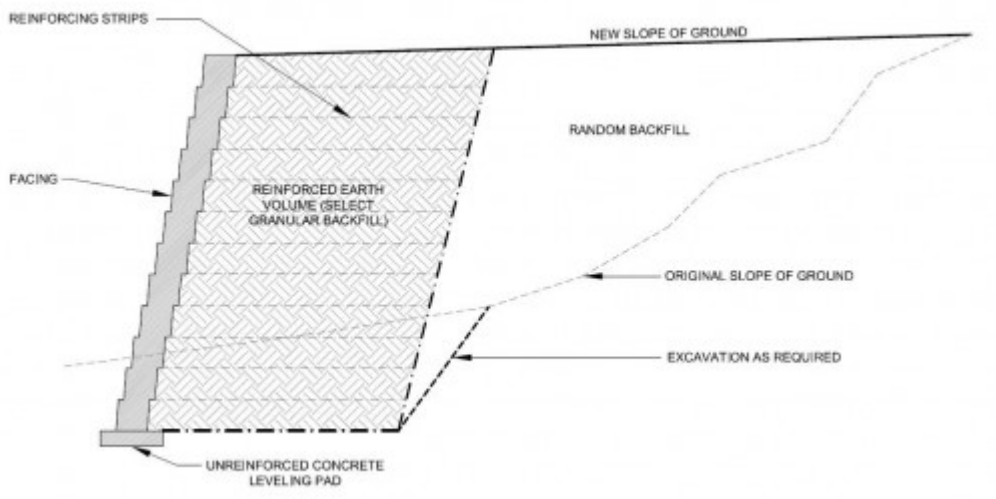

Figure 1.1: Example of a MSE wall.

A MSE wall is one of many types of retaining structures. It classifies as an internally stabilized fill wall, meaning that the wall derives its strength from reinforcement within the soil and is built from the ground up. As shown in Figure 1.1, the wall is constructed with alternating layers of fill and the reinforcing materials. The fill material typically consists of a freely draining granular soil which allows for rapid dissipation of pore pressures upon wetting. The options for the reinforcing material include metallic strips or grids, as well as grids or sheets made from polymeric materials. The decision as to which reinforcement to use will depend on aspects such as environmental conditions and allowable deformations in the wall. Metallic reinforcements are considered to be inextensible, which may reduce wall deformations. A disadvantage of metallic reinforcements is that they are susceptible to corrosion, thereby limiting their applications. The benefits of using polymeric geogrids are price and corrosion resistance. The disadvantage of polymeric reinforcements is that due to the extensibility of the product, greater wall deformations may occur when compared to walls built with metallic reinforcements.

To design a MSE wall, the strength properties of the reinforcement and fill materials are needed, along with the interaction properties between the fill and the reinforcement. Determining the interaction properties is difficult due to lengthy laboratory testing. Being able to extrapolate interaction values from a database of testing results may possibly help with narrowing down the most suitable reinforcement/fill material combinations, thereby reducing the number of tests needed for a design and maximizing the efficiency of the system.

1.2 OBJECTIVES

The objectives of this thesis include the following:

- Collect and organize a broad collection of data in a way that can assist in preliminary selection of interaction properties for uniaxial geogrids;
- Analyze the collection of data for trends related to geogrid polymer type;
- Analyze the collection of data for trends related to the presence of fines in the fill material;
- Compare the collected data to previous studies on the effects of geogrid specimen length on pullout performance; and
- Compare the collected data to previous studies on the effect of geogrid rib thickness to mean particle size ratio on normalized bearing stress and calculated CI values.

1.3 METHODOLOGY

A database was developed to compile the geogrid pullout resistance test results provided by SGI Testing Services, formerly GeoSyntec Consultants (GeoSyntec). The data is contained within 20 reports, each report presenting data for between one to fourteen individual tests. Between July 1992 and December 2000, a total of 101 individual tests were performed on uniaxial geogrids. These tests comprised of 14 different geogrids from five manufacturers, 12 fill materials, and a total of 44 geogrid/fill material combinations. In addition to the pullout resistance testing, the commercial laboratory also performed tests on the fill materials being used to determine the nature and mechanical properties of the soil. From each report, the Coefficient of Interaction (CI) for each geogrid-fill material combination could be calculated. From the database, trends could be observed in the data by querying out the desired parameters and observing the results. Lastly, the data were organized similarly as past studies on

geogrids in an effort to support and possibly elaborate on the effects of geogrid specimen length on pullout performance and the effects of geogrid transverse rib thickness to mean particle size ratio on normalized bearing stress.

1.4 THESIS ORGANIZATION

This thesis is divided into five main chapters. Chapter 2 describes the materials used in the various tests. Chapter 3 discusses the testing apparatus and procedures used while conducting each pullout test, along with a description of the results reported. Chapter 4 presents the findings of the database analysis. It is in Chapter 4 where the general trends and reported CI values for each geogrid/fill material combination can be found. Chapter 5 discusses how the results from this study relate to past studies, and attempts to elaborate on one topic based on the extended set of data available.

Chapter 6 provides a list of conclusions derived from this study.

Appendix A presents the data collected from the pullout testing reports. Appendix B presents the gradation and compaction data for 7 of the 12 fill material tested.

Chapter 2: Material Properties

2.1 GEOGRIDS

Geogrids are reinforcement products made from polymeric materials. Their function is to reinforce soil by intersecting potential failure planes, and distribute load over a larger area than would occur naturally. Geogrids are made from various polymer types including polyester (PET), high density polyethylene (HDPE) and polypropylene (PP). In this study, test results are limited to geogrids made of PET and HDPE. In addition to polymer type, geogrids are categorized by how they are designed to carry load. The categories are uniaxial, biaxial and triaxial. The scope of this study is limited to tests performed on uniaxial geogrids.

HDPE geogrids are typically produced by punching holes into a flat sheet, and then the sheet is stretch to form apertures of various sizes. For uniaxial geogrids, the sheet is only stretched in one direction. This creates a grid pattern with apertures longer in the longitudinal (machine) direction than the transverse (cross machine direction) direction. The longitudinal ribs are more narrow (plan view) and thinner (profile view) than the transverse ribs. The advantages of HDPE uniaxial geogrids are that they can be produced to carry very high tensile loads (in excess of 17,000 lbs/ft), and they are inert in most of the natural conditions where a geogrid would be installed. The disadvantages of HDPE uniaxial geogrids are that they are more rigid than PET which makes them more difficult to place under some conditions, and they experience greater creep than PET. An example of a HDPE geogrid is shown in Figure 2.1.

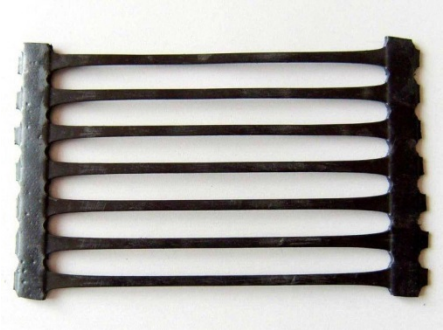

Figure 2.1: HDPE uniaxial geogrid with two transverse ribs running up and down the page and seven longitudinal ribs running across the page.

PET geogrids are produced from woven strands of polyester and are often coated with Polyvinyl Chloride (PVC) for dimensional stability. Unlike the HDPE geogrid, the PET uniaxial geogrids may have longitudinal ribs that are wider than the transverse ribs and the thickness of the longitudinal and transverse ribs are generally similar. Similarly to the HDPE geogrid, the apertures are longer in the longitudinal direction than in the transverse direction. Advantages for using PET geogrids include an even greater tensile load capacity (in excess of 50,000 lbs/ft), greater flexibility and a lighter weight to help with placement. The main disadvantage for PET geogrids is the comparatively higher susceptibility to chemical attack. An example of a PET geogrid is shown in Figure 2.2.

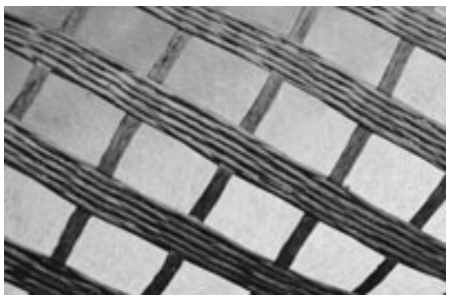

Figure 2.2: PET uniaxial geogrid. Longitudinal ribs shown to be wider than transverse ribs.

Table 2.1 lists the nominal strength and dimension data for some of the uniaxial geogrids tested by GeoSyntec. The data were collected from the manufacturer's website for all geogrids that could be located. Some tests might have been performed on experimental geogrids, therefore no product information is available.

2.2 FILL MATERIALS

A geogrid may perform differently based on the fill material it is placed within. This is the advantage of conducting site-specific testing using the exact geogrid and soil to be used in the construction of a MSE wall. The fill materials used in the database are shown in Table 2.2. These materials include clay, several different sands and graded aggregate base. Soil testing was performed along with the pullout tests in many of the reports available in the database. In some cases though, the soil properties were specified by the client or omitted all together.

Geogrid ID	Polymer Type	Junction Construction	Ultimate Strength	Longitudinal Rib Width	Longitudinal Rib Spacing	Longitudinal Aperture Length	Longitudinal Rib Thickness	Transverse Rib Width	Transverse Rib Spacing	Transverse Aperture Length	Transverse Rib Thickness
			(lbs/ft)	(in)	(in)	(in)	(in)	(in)	(in)	(in)	(in)
PET 1	PET w/PVC	Woven	9500	0.297	1.096	1.315	0.072	0.116	1.431	0.799	0.062
PET 2	PET w/PVC	Woven	3500	0.144	1.113	1.260	0.060	0.126	1.385	0.969	0.061
PET 3	PET w/PVC	Woven	4700	0.196	1.127	1.245	0.059	0.108	1.354	0.931	0.053
PET 4	PET w/PVC	Woven	5900	0.223	1.121	1.214	0.057	0.115	1.330	0.898	0.062
PET 5	PET w/PVC	Woven	7400	0.285	1.237	1.148	0.057	0.117	1.354	0.863	0.058
PET 6	PET	Welded	7192	NA	1.970	4.370	NA	NA	4.720	1.630	NA
PET 7	PET w/PVC	NA	NA	NA	NA	NA	NA	NA	NA	NA	NA
PET 8	PET w/PVC	NA	NA	NA	NA	NA	NA	NA	NA	NA	NA
PET 9	PET w/PVC	NA	NA	NA	NA	NA	NA	NA	NA	NA	NA
PET 10	PET w/PVC	NA	NA	NA	NA	NA	NA	NA	NA	NA	NA
HDPE 1	HDPE	Integrally Formed	4800	0.202	0.910	16.800	0.059	0.796	17.600	0.710	0.137
HDPE 2	HDPE	Integrally Formed	7810	0.207	0.860	17.500	0.083	0.917	18.400	0.650	0.205
HDPE 3	HDPE	Integrally Formed	9870	0.210	0.870	17.800	0.095	0.873	18.700	0.660	0.257
HDPE 4	HDPE	Integrally Formed	11990	0.221	0.870	17.100	0.120	0.830	17.900	0.650	0.325

Table 2.1: Strength and dimension data for tested geogrids.

Soil ID	Soil Description	USCS Soil Class	D_{50}	Average Water Content	Average Unit Weigth	Maximum Unit Weigth	Optimum Water Content	Peak Friction Angle	Peak Cohesion
			(mm)	(%)	(pcf)	(pcf)	(%)	(degrees)	(psf)
Unknown 1	Backfill Soil			15.5	105.5			30	125
Unknown 2	Backfill Soil Submerged			20.5	105.5			30	130
Unknown 3	North Borrow Pit 2			13.7	109.1			39	240
Clay	Clay Lean	CL	0.07	11.5	112.3	118.5	12.5	41	140
Gravel 1	GAB	GW-GM	4.50	1.8	135.0	142.2	5.5	34	0
Gravel 2	GAB 2	GW-GM	5.50	5.5	135.1	142.2	5.5	33	265
Clayey Sand	North Borrow Pit	SC	0.25	14.8	108.1	113.8	14.8	33	165
Silty Sand	Silty Sand	SM	0.25	21.5	93.1	98.0	21.5	34	160
Sand 1	Concrete Sand	SP	0.85	11.0	103.6	109.0	11.0	37	55
Sand 2	Sand	SP		0.0	104.0			34	0
Sand 3	Sand	SP	0.19	0.1	96.0	102.6	11.5	30	10
Sand 4	Sand 3	SP		1.8	104.3				
Sand 5	Sand Dry	SP		2.1	104.5			28	40
Sand 6	Sand Submerged	SP		1.8	104.6			36	45
Sand 7	Well-graded Sand with Silt	SW-SM	0.75	1.2	121.0	124.0	7.8	43	90

Table 2.2: Description, classification and strength data for tested fill materials.

Chapter 3: Geogrid Pullout Testing

3.1 Overview of Geogrid Pullout Resistance Testing

A laboratory pullout test allows for the determination of the CI value between a geogrid and the fill material it will be placed within. The CI is used to determine the required embedment length and spacing of the reinforcement selected for a particular MSE wall design. The CI is calculated using the following equation:

$$CI = \frac{F}{2(A)(\sigma_n tan\varphi + c)} \tag{3.1}$$

where "F" is the maximum pullout load, "2" considers both surfaces of the specimen in contact with the soil, "A" is the embedded area of the geogrid specimen, "σ_n" is the total normal stress applied to the geogrid, "φ" is the friction angle of the fill material, and "c" is the cohesion of the fill material.

The testing apparatus and procedures were performed in general accordance with what is now ASTM D 6706-01 "Standard Test Method for Measuring Geosynthetic Pullout Resistance in Soil."

3.2 Apparatus

To replicate as-built conditions as closely as possible, the Pullout Box was used to measure the pullout resistance of each geogrid. The Pullout Box has the dimensions of 24 inches wide, 84 inches long and 12 inches deep. Normal stress was applied to the soil/geogrid system by means of a pressurized air bladder contained within the box. A load cell was attached to the pullout loading harness to measure the load being applied to the geogrid. Linear variable displacement transducers (LVDTs) were used to measure the

clamp displacement and geogrid displacements. An illustration of a typical pullout box is shown in Figure 3.1.

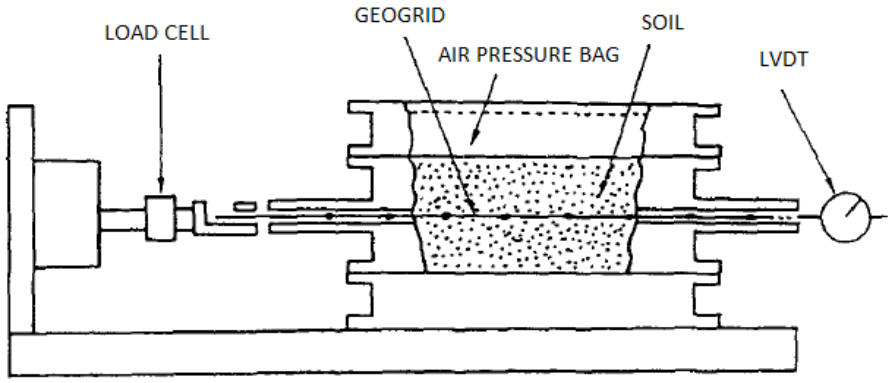

Figure 3.1: Illustration of a typical Pullout Box setup.

3.3 TEST PROCEDURES

A consistent set of procedures were used across all tests. To begin setup, fill material was placed in the pullout box and hand tamped to form a 6 inch layer of soil. The soil was compacted to a predetermined target dry unit weight. Then a virgin geogrid was placed on top of the compacted soil layer and clamped in the pullout loading harness. Tell-tail wires were attached to transverse ribs at one end and to LVDTs at the other end. The tell-tails measured displacement of the geogrid in multiple locations along its length. A second 6 inch layer of compacted soil was then placed on top of the geogrid. Before closing the pullout box with reaction plates, the air pressure bladder was placed on top of the soil. Once the reaction plates were secured, a specified normal stress was applied to the soil/geogrid system by way of the air pressure bladder. After the normal stress was applied, testing began by applying a load to the geogrid through a hydraulic ram which was set at a constant displacement of 0.04 inches per minute. Testing continued until the

pullout load became constant or began decreasing and the transverse rib furthest from the clamp has displaced at least one inch.

3.4 TEST RESULTS

Provided with each report was a summary table detailing the results from each test, and charts illustrating maximum pullout resistance versus normal stress and pullout resistance versus displacement. The details on the summary tables include the following: geosynthetic product tested; geogrid specimen embedded length and width; normal stress applied; and maximum pullout load. An example of a pullout resistance versus displacement chart is shown in Figure 3.2. In this figure, pullout curves from three tests are displayed. Tests from this example were conducted at 0.5, 1.0 and 2.0 pounds per square inch of normal pressure, on geogrid PET 5, in fill material Sand 1.

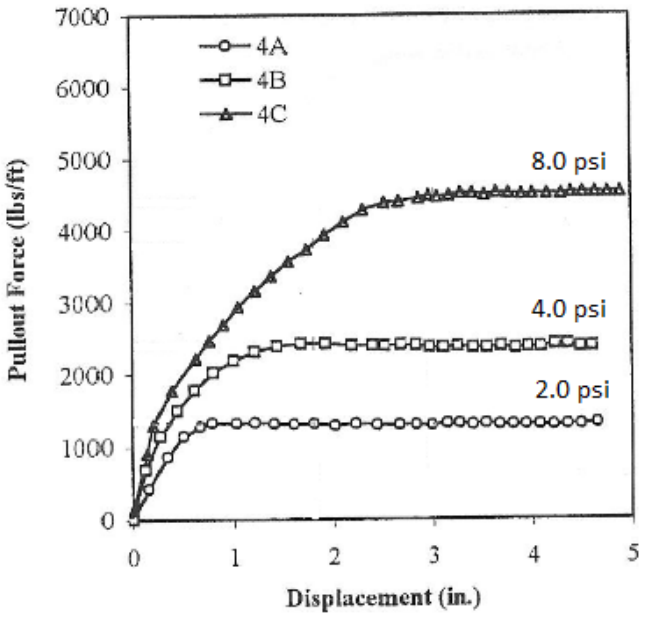

Figure 3.2: Example of a pullout resistance versus displacement chart presented in each report.

Chapter 4: Database Analysis

4.1 DATA SOURCE

Test results were obtained from 20 testing reports, which comprised of 44 different geogrid/fill material combinations, making up 101 individual pullout resistance tests. In addition to the pullout resistance test data, direct shear tests were performed to determine the mechanical properties of 12 fill materials, and 9 of those 12 had soil index properties determined. The selected data from each of these tests were entered into an Access database, which was built specifically for this study.

Data collected from each pullout resistance test includes the following: geogrid model, fill material, displacement rate (equal to 0.04 inches per minute in all cases), geogrid specimen embedded length and width, normal stress applied, maximum pullout resistance, and the reported CI.

Data collected on each fill material from the direct shear and index properties tests includes the following (if available): soil description, Unified Soil Classification System (USCS) classification, mean particle size (taken as the D_{50}), testing water content, optimum water content, compacted dry unit weight, maximum dry unit weight, peak friction angle and peak cohesion. Fill material information is presented in Table 2.2.

Little to no information was provided within the reports about the geogrids being tested. Data sheets from the geogrid manufacturer's websites provided dimensions for 9 out of the 14 geogrids tested. Data sheets from three manufacturers were unavailable. Data collected on each geogrid includes the following: manufacturer, model, polymer type, junction type, and longitudinal and transverse rib dimensions (width, spacing and thickness). The geogrid information can be found on Table 2.1. Product names and manufacturer information have been removed from the listed tables since the intension of this study is to be broader in nature.

4.2 SUMMARY OF TEST RESULTS

One of the goals of this thesis is to present the results from geogrid pullout resistance tests, performed on a fairly wide range of geogrid/fill material combinations, so that CI values can be interpolated for use in preliminary designs of MSE walls. As presented in Figure 4.1 for the case of geogrid HDPE 1, the data have been organized by geogrid, displaying CI versus normal stress for each fill material in which it was tested. In this figure, the testing results for geogrid HDPE 1are displayed for the six different fill materials with which it was tested.

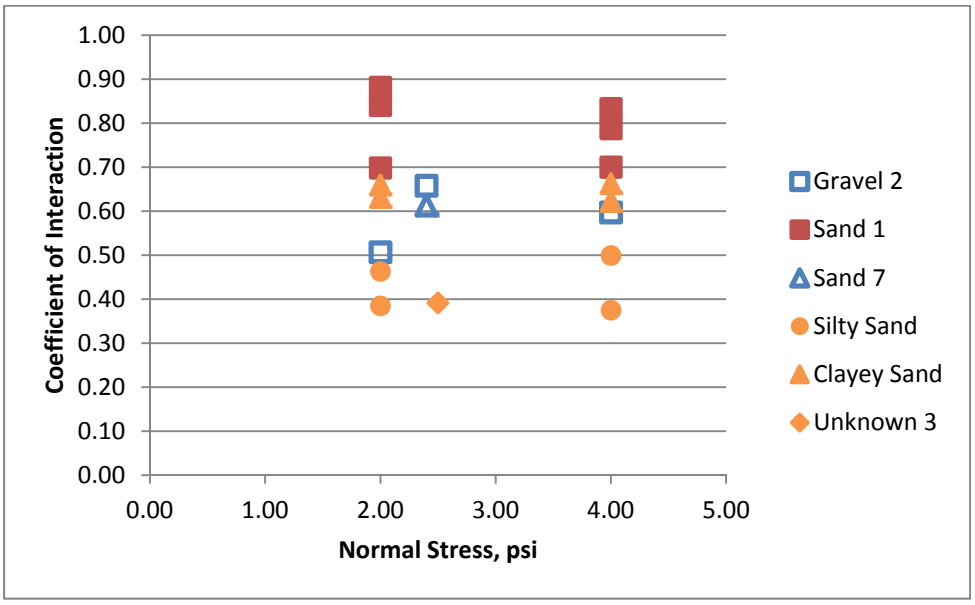

Figure 4.1: Sample chart of geogrid test results.

Figures A.1 through A.14 in Appendix A illustrate this information for all 14 geogrids. This data is also shown in tabular format in Table A.1 in Appendix A. Descriptions for geogrids and fill materials are found in Table 2.1 and Table 2.2 respectively.

4.3 ANALYSIS OF RESULTS

General trends and observations were evaluated during the database analysis. These include the effects of geogrid polymer type, specimen length and presences of fines in the fill material.

4.3.1 Effects Geogrid Polymer Type

Figure 4.2 presents the general trends for CI versus normal pressure for all of the HDPE geogrids (HDPE 1 through 4) tested, grouped by fill material. To view the individual performance of each geogrid separately, please refer to Figure A.11 through A.14 in Appendix A.

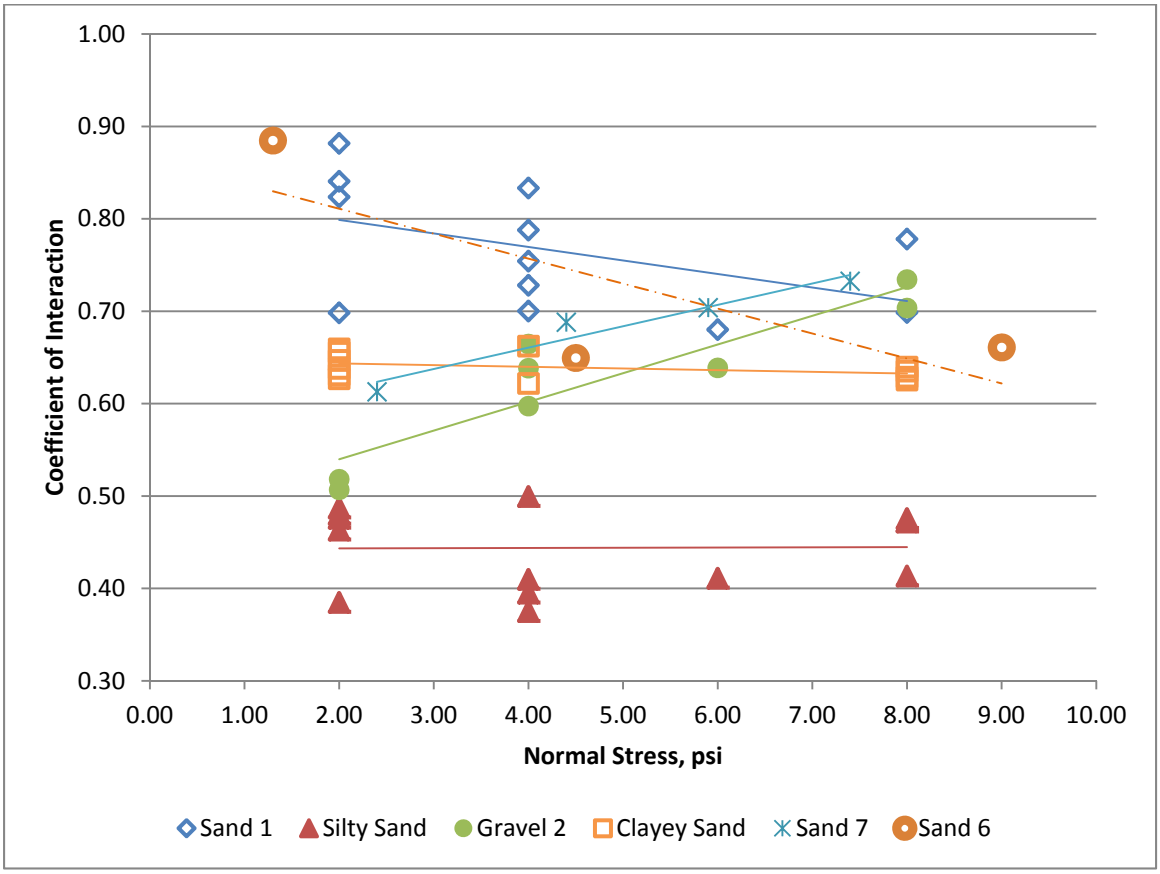

Figure 4.2: Results of HDPE geogrids tested in various fill materials.

Figure 4.2 illustrates the following trends for the HDPE geogrids: increasing CI trends are observed for Sand 7 (well graded silty sand) and Gravel 2, level trends (CI independent of normal stress) observed for Clayey Sand and Silty Sand and decreasing CI trends observed for Sand 1 and Sand 6 (Sands 1 and 6 are poorly graded sands). CI values range from 0.38 to 0.88 or the normal stress range of 1.3 to 9.0 psi.

Figure 4.3 presents the general trends for CI versus normal pressure for all of the PET geogrids (PET 1 through 10) tested, grouped by fill material. To view the individual performance of each geogrid separately, please refer to Figure A.1 through A.10 in Appendix A.

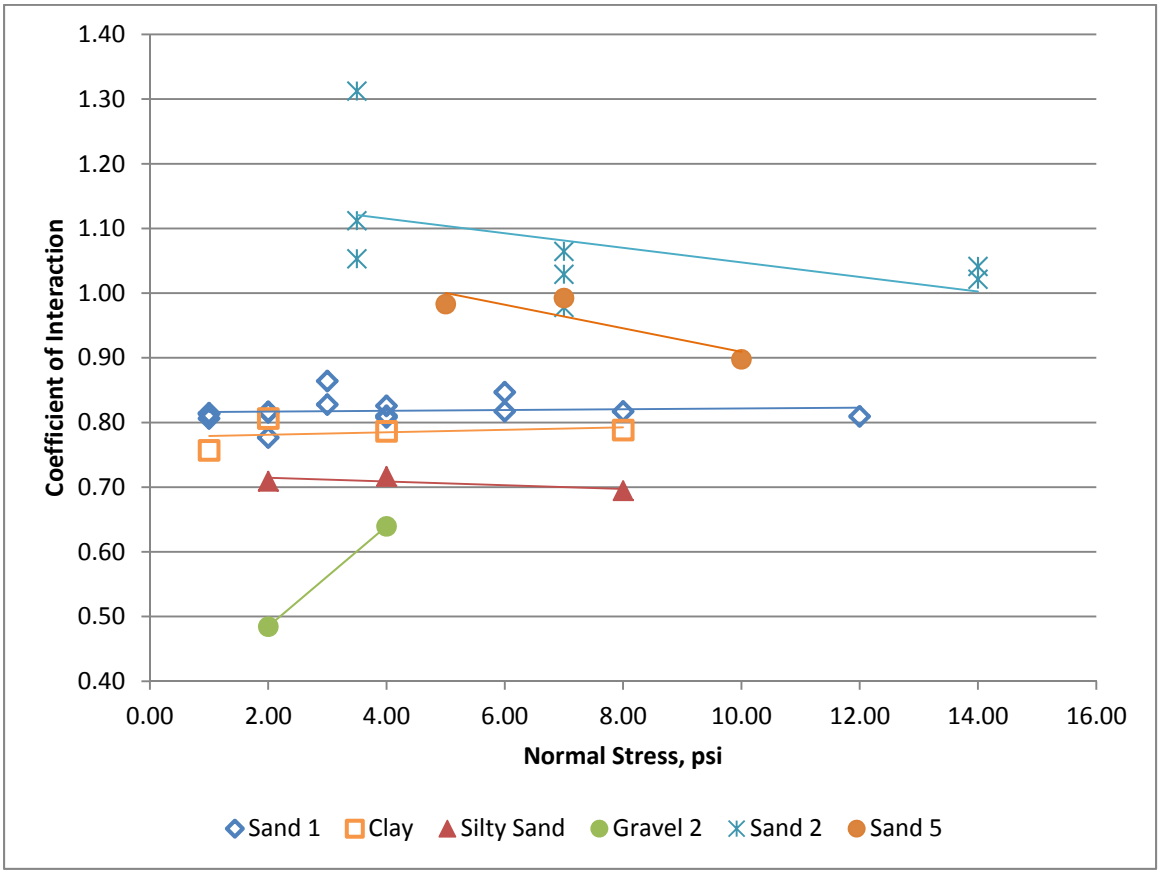

Figure 4.3: Results of PET geogrids tested in various fill materials.

Figure 4.3 illustrates the following trends for the PET geogrids: an increasing CI trend is observed for the Gravel 2 material, nearly level CI trends observed for Sand 1, Clay, and Silty Sand, and decreasing CI trends observed for Sand 2 and Sand 5 (Sands 2 and 5 are poorly graded sands). CI values range from 0.48 to 1.31 over the normal stress range of 1.0 to 14.0 psi.

Three fill materials were tested with both polymer types. These fill material were Sand 1, Silty Sand and Gravel 2. Differing responses are shown by the polymer types tested in Sand 1 (poorly graded sand). The CI value for PET geogrids in Sand 1 remain unaffected by increasing normal stress, while the HDPE geogrids exhibit a decreasing trend with increasing normal stress. Sand 2, Sand 5 and Sand 6 are also poorly graded sands. The PET and HDPE geogrids in these three sands show decreasing trends. A comparison of the geogrids tested in Sand 1, Sand 2, Sand 5 and Sand 6 can be seen in Figure 4.4. In this figure, the PET geogrids in Sand 2 are denoted with orange symbols, the PET geogrids in Sand 5 are denoted with purple symbols, the PET geogrids in Sand 1 are denoted with red symbols, the HDPE geogrids in Sand 1 are denoted with blue symbols, and the HDPE geogrids in Sand 6 are denoted with green symbols. The individual geogrids are identified in the legend.

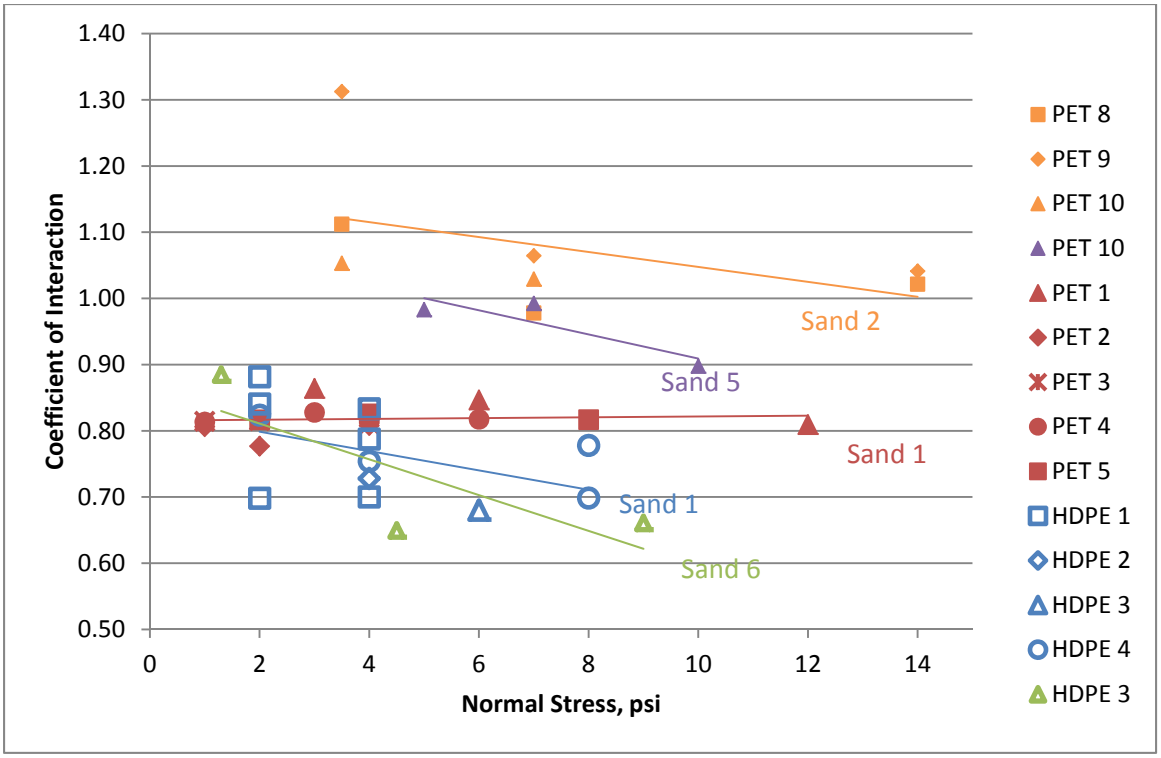

Figure 4.4: Comparison of HDPE and PET geogrids performance in Sand 1, Sand 2, Sand 5 and Sand 6 fill materials.

Decreasing trends in CI for poorly graded sand have been shown in literature as well. In Figure 4.5, Moraci (Moraci, 2006) shows a decreasing trend in apparent friction angle for increasing normal stress. In this figure the apparent friction angles for geogrids of different lengths are being compared with increasing normal stress. Also shown in this figure is the tangent of the soil friction angle plotted against the normal stress. Moraci explains that larger apparent friction angles are observed at lower vertical stresses than at higher vertical stresses due to the dilatancy effect in sands. The increased change in volume of the sand, in the immediate area of the geogrid, is responsible for the increase in apparent friction angle. The dilatancy effect is suppressed with increasing vertical stress.

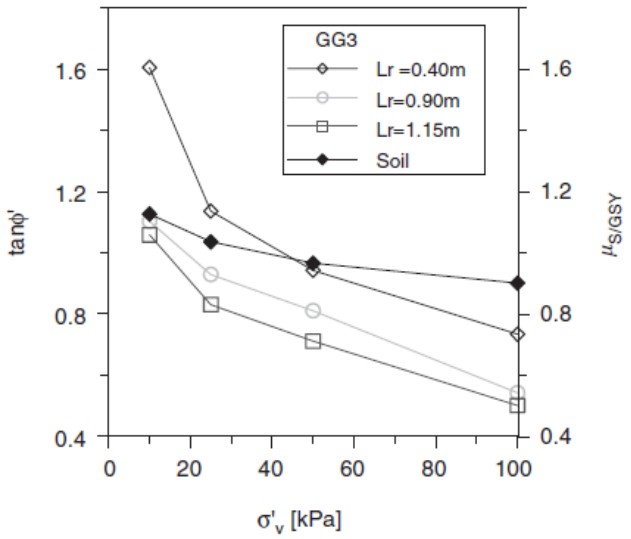

Figure 4.5: Example from literature (Moraci, 2006). Decreasing CI with increasing normal stress for HDPE geogrids in poorly graded sand.

The results for both polymer types tested in the Silty Sand fill material exhibit similar trends. The trends show a CI value that remains independent of normal stress across the pressures tested. Similar trends are seen in fill materials Clay and Clayey Sand. Common to each of these tests is the presence of fines content in the fill material that are greater than 12%, which could help to link these trends. The effects of the presence of fines in fill material are discussed in more detail later in this chapter. A comparison of geogrids in these three fill materials is shown in Figure 4.6. PET geogrids tested in Clay are denoted with green symbols, PET in Silty Sand are denoted with red symbols, HDPE in Clayey Sand are denoted with orange symbols and HDPE in Silty Sand are denoted with blue symbols. Individual geogrids within each soil group are shown in the legend.

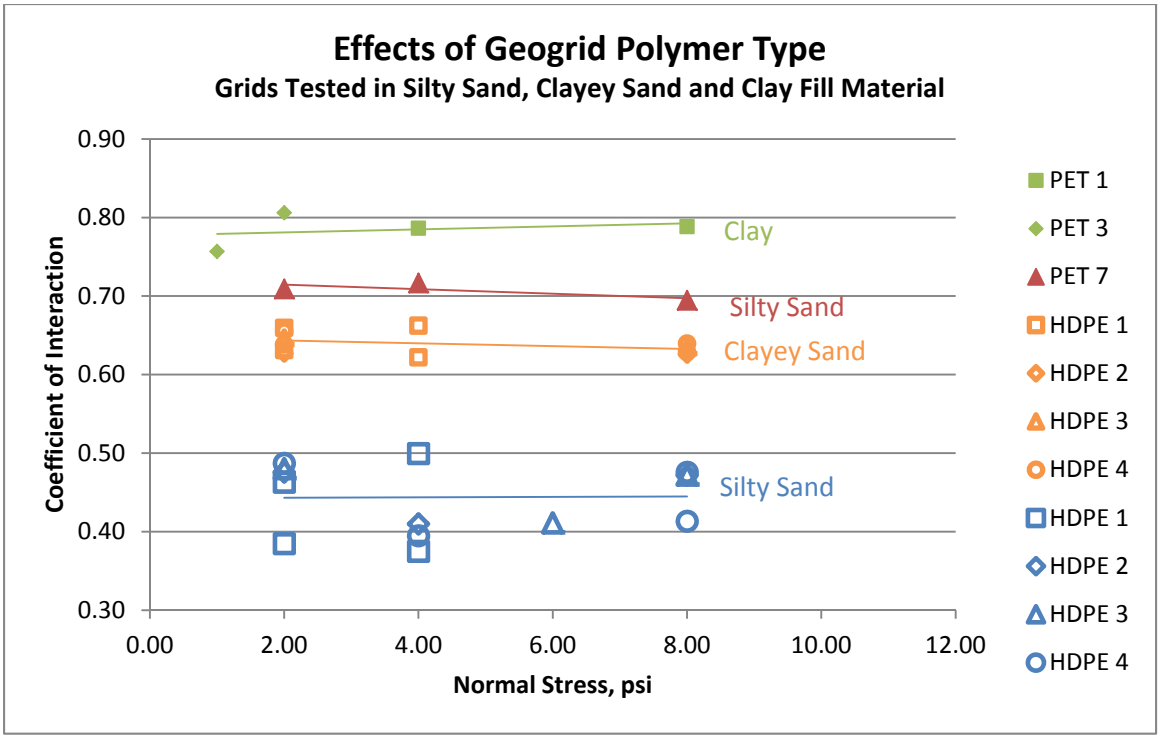

Figure 4.6: Comparison of HDPE and PET geogrids performance in Clay, Silty Sand and Clayey Sand fill materials.

The results for both polymer types tested in Gravel 2 fill material also exhibit similar trends. An increasing trend with increasing normal stress is exhibited for this material. The trend for Sand 7 follows a similar pattern. Common to Gravel 2 and Sand 7 is that each fill is a well graded material. Well graded soils typically have a greater shear strength than poorly graded soils due to increased surface contact of soil particles. It could be speculated that the well graded soils are better able to fill in the geogrid openings, increasing the amount of soil available to apply passive pressure to the transverse members. A comparison the geogrids tested in Gravel 2 and Sand 7 is shown in Figure 4.7. HDPE geogrids in Sand 7 are denoted with blue symbols, HDPE geogrids

in Gravel 2 are denoted with red symbols and PET geogrids in Gravel 2 are denoted with green symbols. Individual geogrids within each soil group are shown in the legend.

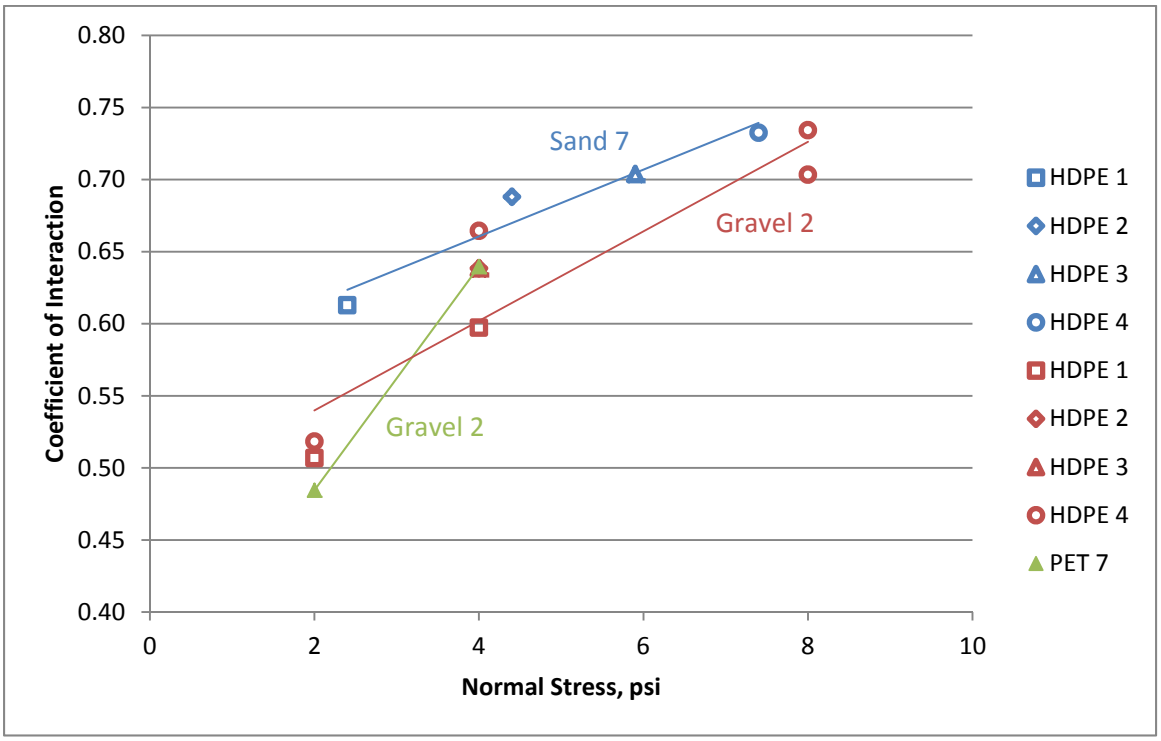

Figure 4.7: Comparison of HDPE and PET geogrids performance in Sand 7 and Gravel 2 fill materials.

Comparison of actual CI values between the two geogrid materials is difficult due to the specimen lengths used for each type. The HDPE geogrids were typically tested with a 70 inch specimen, while the PET geogrids were tested at an average length of 42 inches. Shorter specimen lengths typically produce greater CI values due to the extensibility of geosynthetics. The effects of specimen length on pullout resistance are discussed in greater detail in Chapter 5.

4.3.2 Effects of the Presence of Fines in Fill Material

The effects of the presence of a significant amount of fines in the fill material were analyzed for both PET and HDPE geogrids. A significant amount of fines is defined in this study as greater than 12% by weight, consistent with the Unified Soil Classification System definition of a dirty granular soil. Three fill materials met this definition, which are Clay, Clayey Sand and Silty Sand. All other fill materials had less than 12 % fines (of the soils we had gradation data on). The typical response of a HDPE geogrid within a poorly graded clean granular fill material is a decrease in CI with increasing normal stress. This can be seen with the trend shown for geogrids in Sand 1 (blue series) on Figure 4.8. The trends for HDPE tested in Clayey Sand and Silty Sand show a relatively flat response, having no significant increase or decrease in CI with increased normal stress. CI values for HDPE geogrids in fill materials with significant fines content are shown here to be lower than values in a clean granular fill. CI values in the Clayey Sand fill material are between 10% and 28% lower than values in Sand 1. CI values in the Silty Sand fill material are between 33% and 57% lower than values in Sand 1. Comparisons are made over the normal stress range of 2.0 to 8.0 psi. In Figure 4.8 grouping by fill material is by color (Sand 1 is blue, Clayey Sand is orange, and Silty Sand is red), while grouping by geogrid is by symbol shown in the legend.

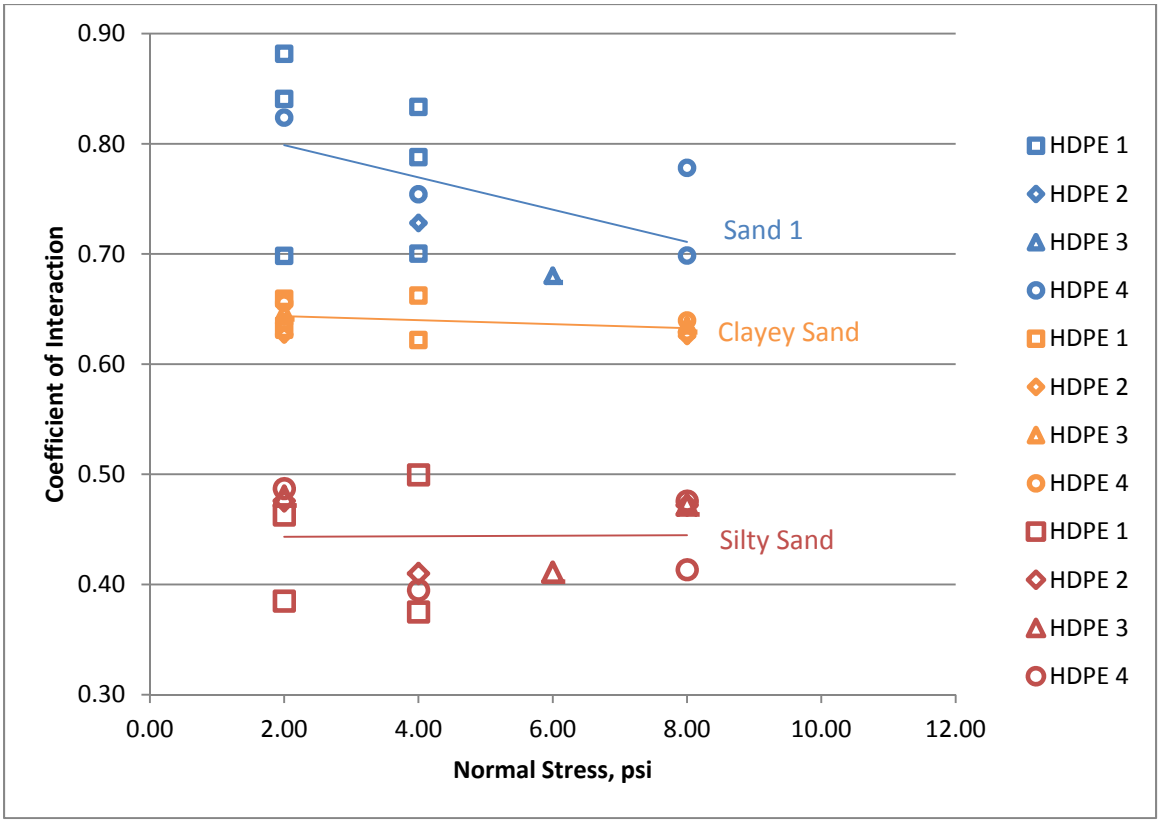

Figure 4.8: Effects of the presences of fines in fill material on the CI value for HDPE geogrids.

The PET geogrids tested in poorly graded clean granular fill material show little to no change in CI value with increasing normal stress. This can be seen with the trend shown for the geogrids in Sand 1 (blue series) on Figure 4.8. For the PET geogrids tested, the presence of fines tends to produce similar results as with Sand 1. A comparison of geogrids tested in Sand 1, Clay and Silty Sand is shown in Figure 4.9. As with the HDPE geogrids, the presences of fines in the fill material reduce the actual CI value. CI values in the Clay fill material are between 4% and 6% lower than values in Sand 1. CI values in the Silty Sand fill material are between 16% and 26% lower than values in Sand 1. Comparisons are made over the normal stress range of 1.0 to 8.0 psi. In Figure 4.9

grouping by fill material is by color (Sand 1 is blue, Clay is green, and Silty Sand is red), while grouping by geogrid is by symbol shown in the legend.

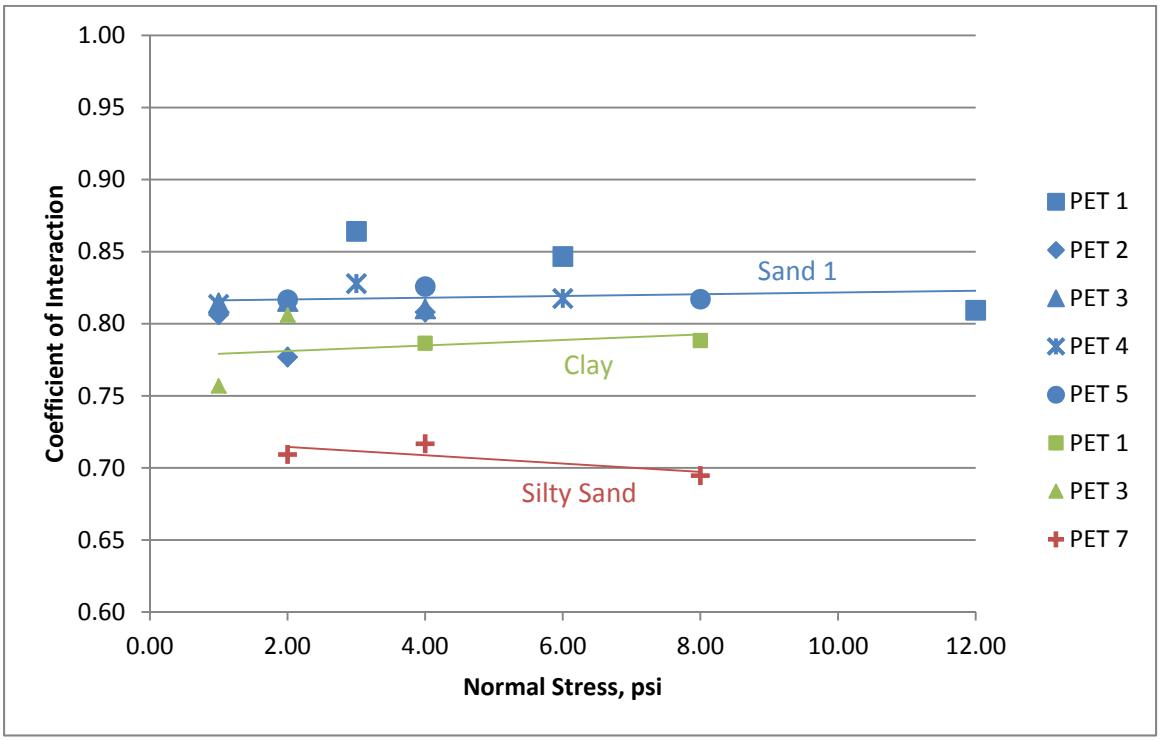

Figure 4.9: Effects of the presences of fines in fill material on the CI value for PET geogrids.

The presence of a significant percentage of fines (>12%) are shown to produce a decrease in calculated CI for all geogrids tested.

Chapter 5: Additional Parametric Evaluations

5.1 Effects of Geogrid Specimen Length on Pullout Performance

The effects of embedment length on pullout behavior have been studied by N. Moraci (Moraci, 2006). His research included testing the same geogrid at different specimen lengths to see how each performed. The results showed that while specimens with longer lengths had greater pullout resistance, it was the shorter sample that carried the greatest load per unit surface area. Figure 5.1 is comprised of two charts, each for a different geogrid. On each chart, pullout test results are plotted for three specimen lengths (0.40 m, 0.90 m, and 1.15 m). These charts illustrate that the shortest specimen (denoted with circle symbol) carried the greatest load per unit area.

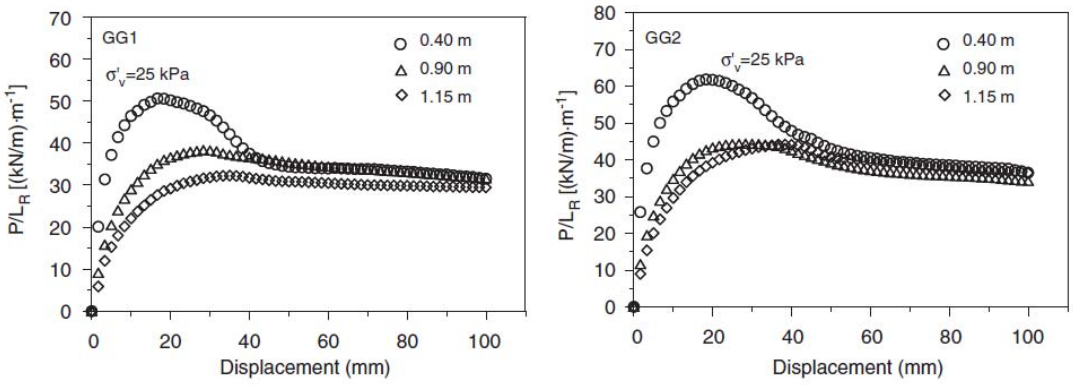

Figure 5.1: Figures from (Moraci, 2006), showing pullout resistance normalized by specimen length.

The effect of specimen length is likely due to the extensibility of geosynthetic geogrids. In Figure 5.1, the 0.40 meter sample shows significant strain softening. This occurs because all (or most) of the bearing members mobilize bearing capacity at the same time. After reaching a maximum capacity, the bearing resistance reduces to a residual value. As the sample lengths are increased (0.90 and 1.15 meters), the strain softening effect diminishes. An explanation for this behavior could be that as the geogrid

stretches under tension, bearing members are being engaged at different times and rates. So as one bearing member is reaching maximum capacity, the bearing member before it is likely past maximum capacity (maybe nearing residual capacity), and the bearing member after it may have only mobilized a very small portion of maximum capacity.

Data from this study exhibit similar trends as what is shown in Moraci's work. Figure 5.2 illustrates the pullout curves (pullout resistance versus displacement) for eight separate geogrid tests from the database. These tests were conducted using four different HDPE geogrids (one color for each model), the same fill material (Gravel 2) for all tests, and 2 different embedment lengths per model (40 inches and 70 inches). The results show a pullout resistance which is greater for the 70 inch sample (lines marked with triangles) than for 40 inch samples (lines marked with circles).

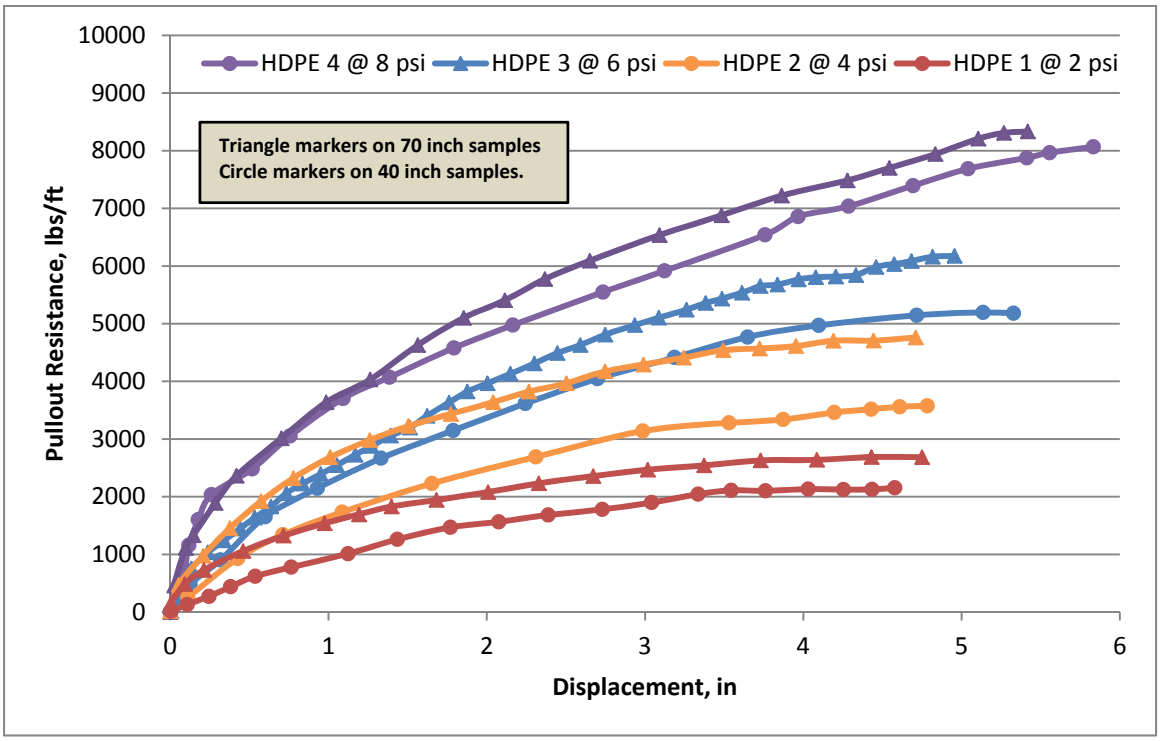

Figure 5.2: Pullout curves for HDPE geogrids showing the effect of specimen length on pullout resistance.

Figure 5.3 illustrates the same data, but the pullout resistance is normalized by the specimen length. It is clear that the shorter specimens carry a greater load per unit area. Data collected from each of these figures are summarized in Table 5.1. In this table, the maximum pullout resistance for the 40 inch samples and 70 inch samples are listed along with the percent change going from the 40 inch to the 70 inch results. The same is listed for the normalized pullout resistance.

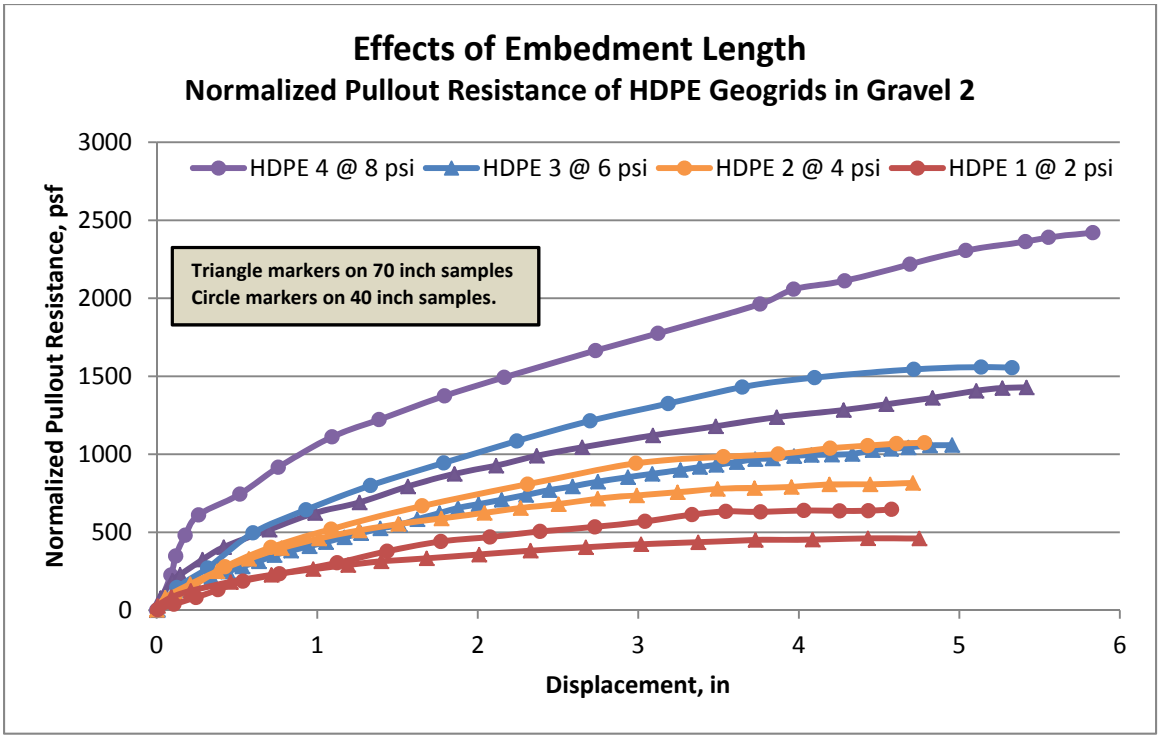

Figure 5.3: Pullout curves for HDPE geogrids showing the effect of specimen length on normalized pullout resistance.

Table 5.1: Summary of pullout results for specimens of different length, pullout resistance and pullout resistance normalized by specimen length.

Geogrid	Pullout Resistance			Normalized Pullout Resistance		
	Max 40" (lbs/ft)	Max 70" (lbs/ft)	% Change	Max 40" (psf)	Max 70" (psf)	% Change
HDPE 1	2154	2687	25%	646	461	-29%
HDPE 2	3577	4760	33%	1073	816	-24%
HDPE 3	5196	6175	19%	1559	882	-43%
HDPE 4	8068	8333	3%	2420	1429	-41%

Figure 5.4 presents the CI values calculated for each test shown in Figure 5.2. The results from both specimen lengths show an increasing trend with increasing normal stress, and appear to converge at low confining pressures. The rate (CI/psi) at which the 40 inch samples increase is greater than the rate at which the 70 inch samples increase. Specimen length is shown to have a significant effect on calculated CI values at high confining pressures. This was the only geogrid/fill material combination that had more than one sample length tested. Figure 5.4 groups the data by specimen length using color (blue for 40 inch specimens and red for 70 inch specimens), and by geogrid using symbols in the legend.

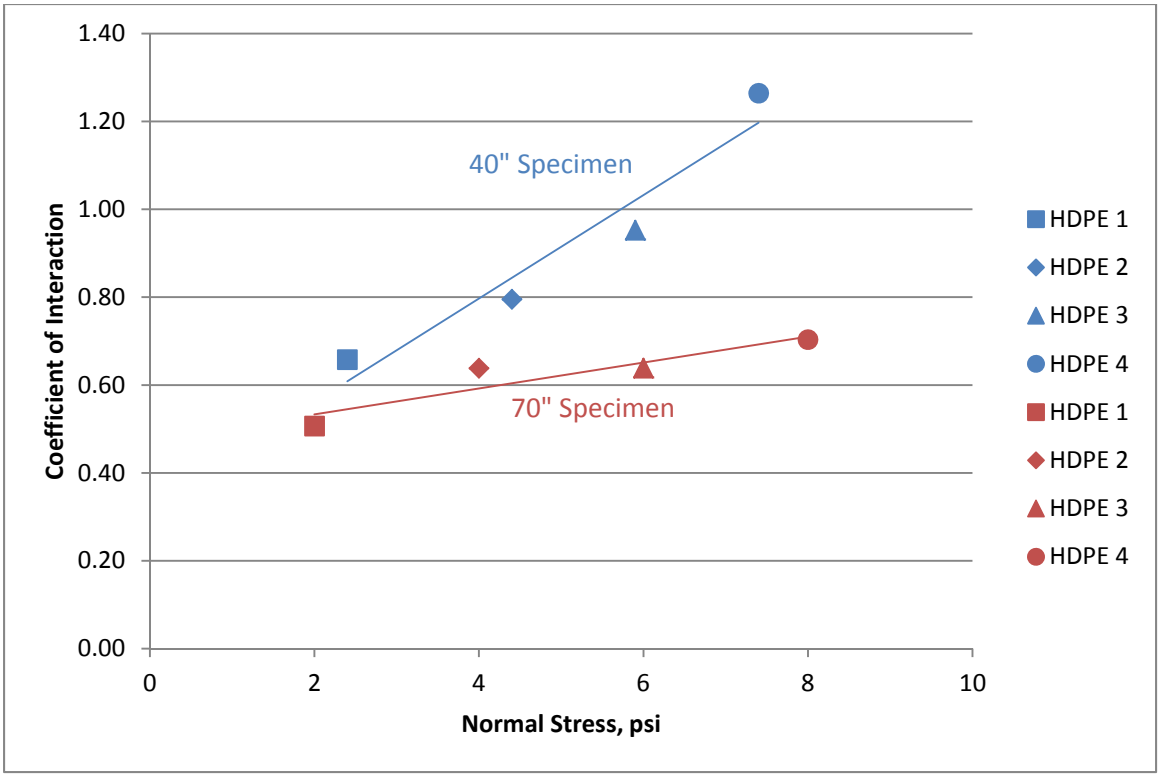

Figure 5.4: HDPE geogrids tested in Gravel 2 fill material, 40” and 70” samples.

5.2 SOIL-GRID INTERACTION WITH REFERENCE TO BEARING STRESS

Geogrid anchorage strength is derived through two components, skin friction and bearing resistance. The skin friction develops between the geogrid and fill material, which mainly occurs on the top and bottom surface area of the longitudinal ribs. The bearing resistance develops at the leading face of each transverse rib. With tests performed on individual longitudinal and transverse ribs, S. H. C. Teixeira (Teixeira, 2007) states that approximately 60% of the pullout resistance comes from the transverse ribs. These tests were performed on PVC coated PET geogrids.

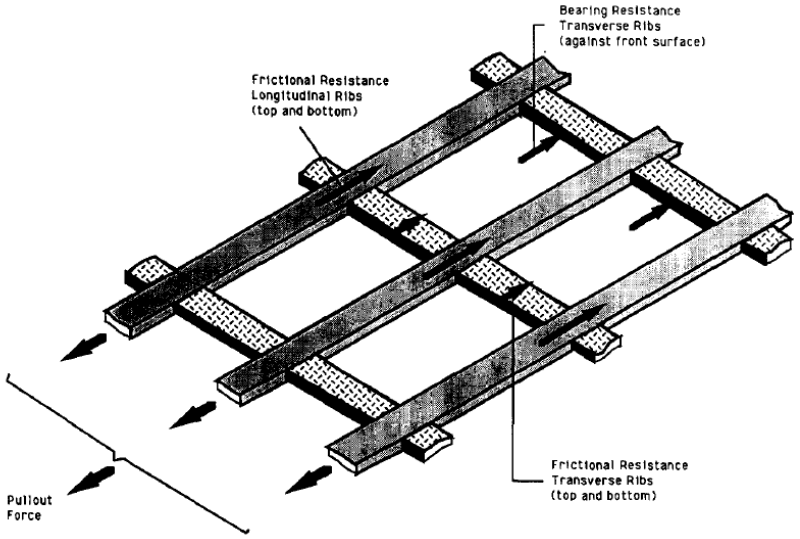

Figure 5.5: Illustration of components of resistance to pullout force (Koerner, 1993).

Earlier studies by R. M. Koerner (Koerner, 1993) show a similar proportion of load carried by the transverse rib. In Figure 5.6, the percentage of each component of resistance is plotted against the percentage of ultimate pullout force. As the load increases from zero to 100% of ultimate pullout force, the proportion of friction resistance to bearing resistance begins to drop. Koerner explains that this is to be expected since the displacements required to mobilize shear resistance are much lower than the displacements required to mobilize bearing resistance.

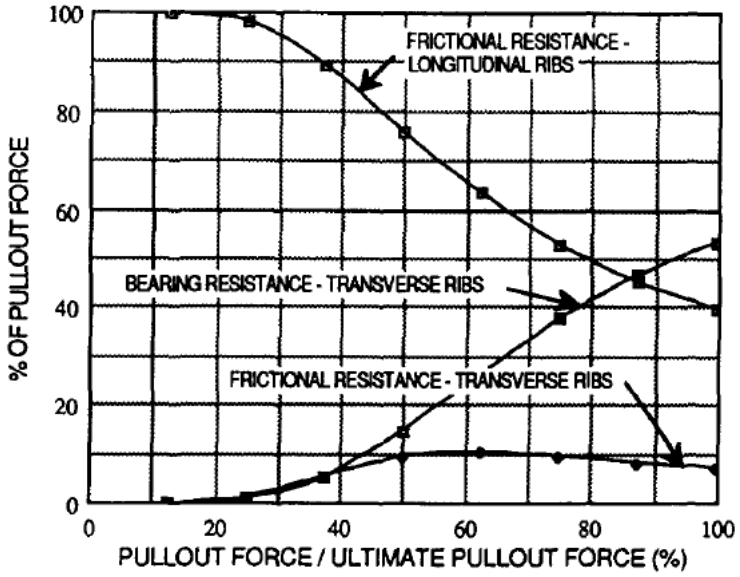

Figure 5.6: Graph of components of resistance to pullout force (Koerner, 1993).

Since the majority of the resistance against pullout is developed along the transverse rib, it is important to understand the soil-grid interaction along this zone. E. M. Palmeira (Palmeira, 1989) discusses how the transverse rib thickness (B) to mean soil particle diameter (D_{50}) ratio affects pullout. Palmeira states that it is improper to estimate bearing stresses using equations derived for a continuum when B/D_{50} is smaller than 15. The value of 15 comes from the data shown on Figure 5.7. Palmeira states that the data shown on Figure 5.7 is likely not unique for all sands.

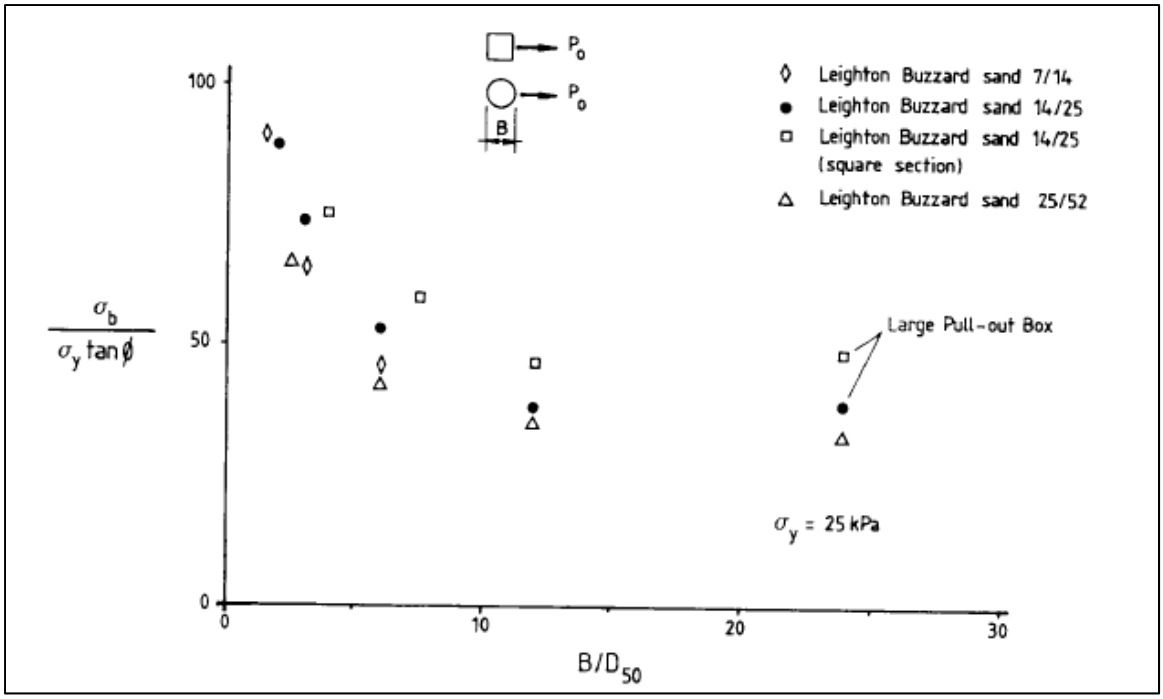

Figure 5.7: Normalized bearing stress versus transverse rib thickness to mean soil particle diameter (B/D_{50}) for metal grids in sand, (Palmeira, 1989).

The graph in Figure 5.7 compares the normalized bearing stress to B/D_{50}. The normalized bearing stress is calculated using Equations 5.1 and 5.2. Equation 5.1 calculates the bearing stress on the leading face of a transverse rib. Equation 5.2 calculates the normalized bearing stress.

$$\sigma_b = \frac{P_0}{B * W_r} \tag{5.1}$$

$$Normalized\ Bearing\ Stress = \frac{\sigma_b}{\sigma_y * tan\varphi + c} \tag{5.2}$$

where "P_o" is the maximum pullout force, "B" is the rib thickness, "W_r" is the width of the rib being tested, "σ_y" is the normal stress applied, "φ" is the peak friction angle of the soil and "c" is the peak cohesion of the soil.

The results from Palmeira's study shows that a decreasing trend in normalized bearing stress occurs with increasing B/D_{50} for B/D_{50} values less than 15. For B/D_{50} values greater than 15, normalized bearing stress acts independent of B/D_{50}.

The database of test results was analyzed to view how well this concept applies to extensible geogrids and various fill materials. A number of assumptions were made to compare these data to Palmeira's results. The goal of this analysis is to identify trends in the data rather than predicting actual bearing stress. Since the proportion of skin friction resistance to bearing resistance is unknown, 100% of the pullout resistance is assumed to be provided by bearing resistance. Since Palmeira's tests were performed on single transverse ribs, the pullout force per transverse rib was calculated using Equation 5.3.

$$P_o = \frac{P_{ult} * W}{N_{trans}} \tag{5.3}$$

where "P_{ult}" is the maximum pullout resistance measured for multi rib specimen, "W" is the width of the sample and "N_{trans}" is the number of transverse ribs along the sample. The area of the leading face of each transverse rib was calculated using Equation 5.4.

$$A_{face} = W * B - A_{long} * N_{long} \tag{5.4}$$

where A_{long} is the area of the longitudinal ribs and N_{long} is the number of longitudinal ribs across the specimen. The bearing stress was calculated using Equation 5.5.

$$\sigma_b = \frac{P_o}{A_{face}} \tag{5.5}$$

The normalized bearing stress was calculated using Equation 5.2. Test results from the four HDPE geogrids were used in this analysis due to the varying rib thicknesses across specimens.

Figure 5.8 illustrates the results of this analysis, grouped by fill material. Since the data are grouped by fill material (constant D_{50}), changes in B/D_{50} are due to the various geogrid rib widths tested within the fill material. General trend lines are included to identify how the normalized bearing stress varies with B/D_{50} for each fill material. Palmeira's results are also shown for reference. Similar to Palmeira's data, the trend shows a decrease in normalized bearing stress with increasing B/D_{50} for each fill material. Unlike Palmeira's data is that each material appears to exhibit a continuous decrease across all values of B/D_{50} tested. Based on the results shown in Figure 5.8, the normalized bearing stress becomes more sensitive to changes in B/D_{50} as the D_{50} of the soil increases.

By increasing the resolution and focusing on the results of each material separately revealed a slight difference only in the Gravel 2 tests. In Figure 5.9, two different trends are noted. The difference between the two test series was the geogrid sample embedment length. The test series with 40 inch long samples exhibit a trend similar to Palmeira's data, while the test series with 70 inch samples exhibit a trend similar to the remaining tests in this study, which also had 70 in samples. As shown in Figure 5.4 and again in Figure 5.9, the sample length can have a significant effect on test results.

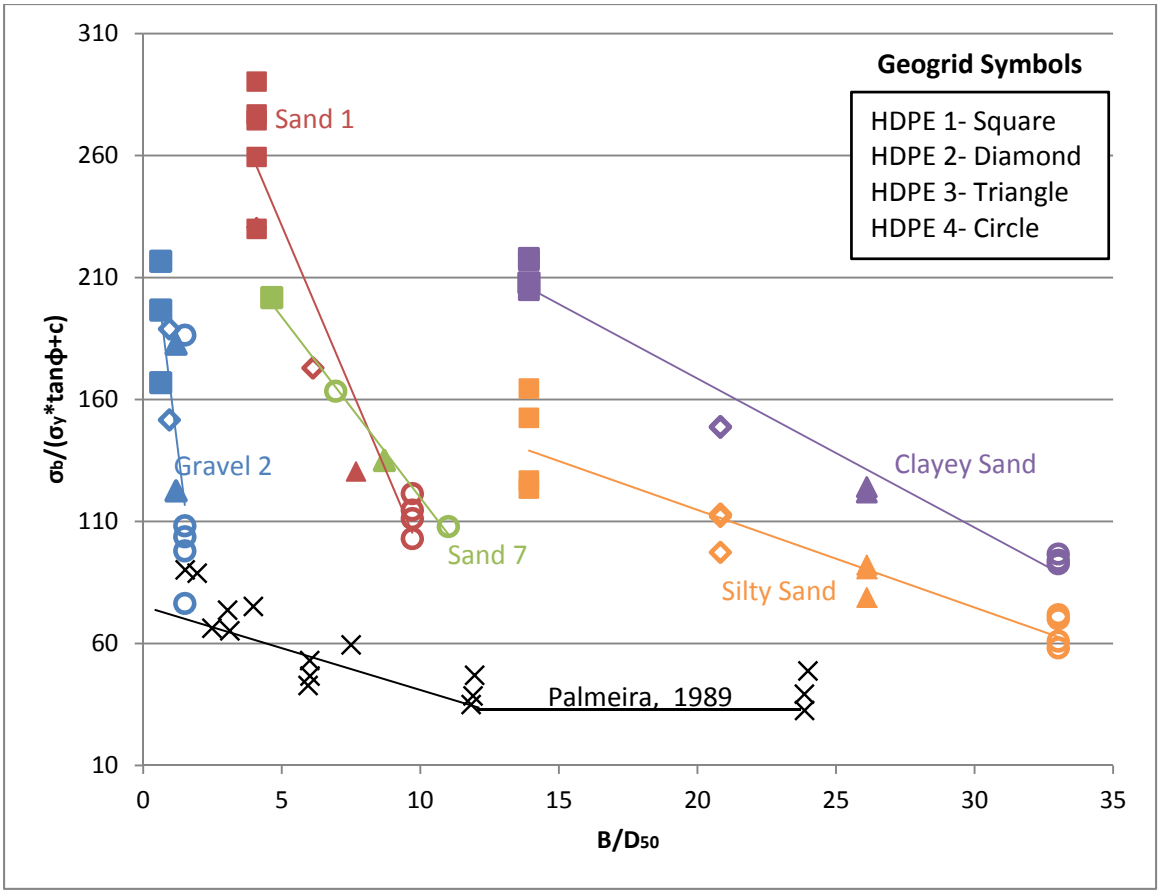

Figure 5.8 Influence of the transverse rib thickness to mean particle diameter ratio on normalized bearing stress, by specific soil.

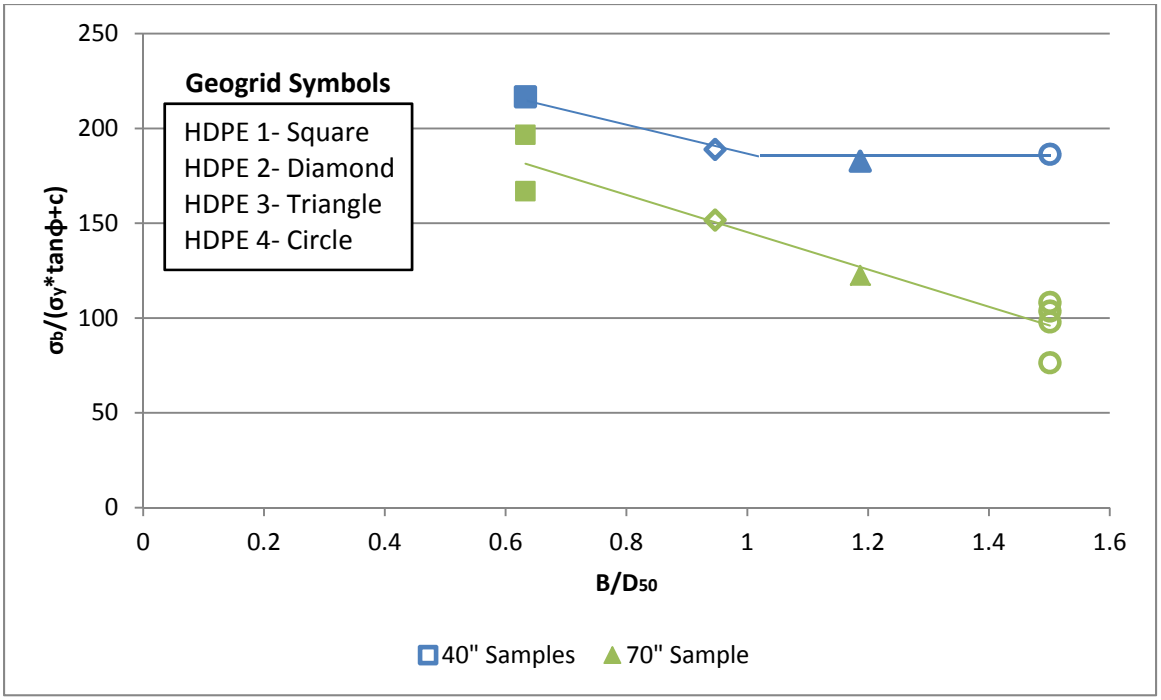

Figure 5.9 Influence of the ratio transverse rib thickness to mean particle diameter on bearing stress for two different length geogrids in Gravel 2 fill material.

In Figure 5.8, the trends shown for specific fill materials. Figure 5.10 illustrates the trends for specific geogrid models (constant B). Now changes in B/D_{50} are the result of the various mean particle sizes of the different fill materials in which the geogrid was tested. As seen in Figure 5.10, the data for three of the four geogrids (HDPE 1, HDPE 2 and HDPE 4) exhibit either an increasing or constant normalized bearing stress for B/D_{50} values from zero to somewhere between 5 and 10. In this B/D_{50} range a peak occurs, and then a decreasing trend develops with increasing B/D_{50}. Palmeira suggests for a grid being forced through sand, the failure mechanism shifts from a punching shear to a general shear at a B/D_{50} value of 7.5. This shift in failure mechanism might explain the shift from increasing to decrease trends shown in Figure 5.10. From these trends it could be speculated that an optimum value of D_{50} exists for a given geogrid. Based on the test

results in this analysis, a B/D_{50} value between 5 and 10 appears to be the optimum range for the geogrids tested.

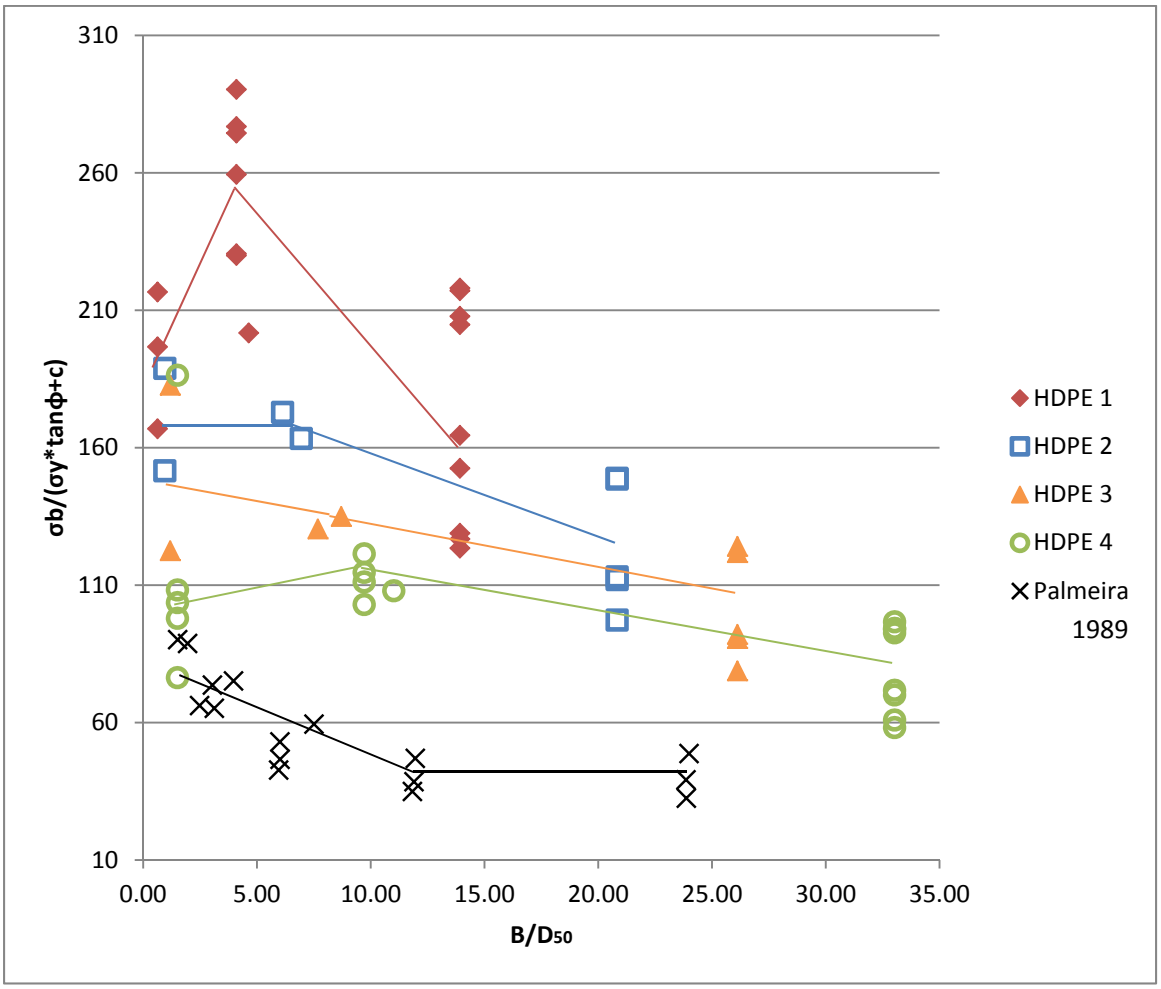

Figure 5.10 Influence of the ratio transverse rib thickness to mean particle diameter on normalized bearing stress, by specific geogrid.

In Figure 5.11, the calculated CI values were plotted against B/D_{50}. The data follow very similar trends as those shown on Figure 5.10, reinforcing the concept of an optimum particle size for a given geogrid rib width.

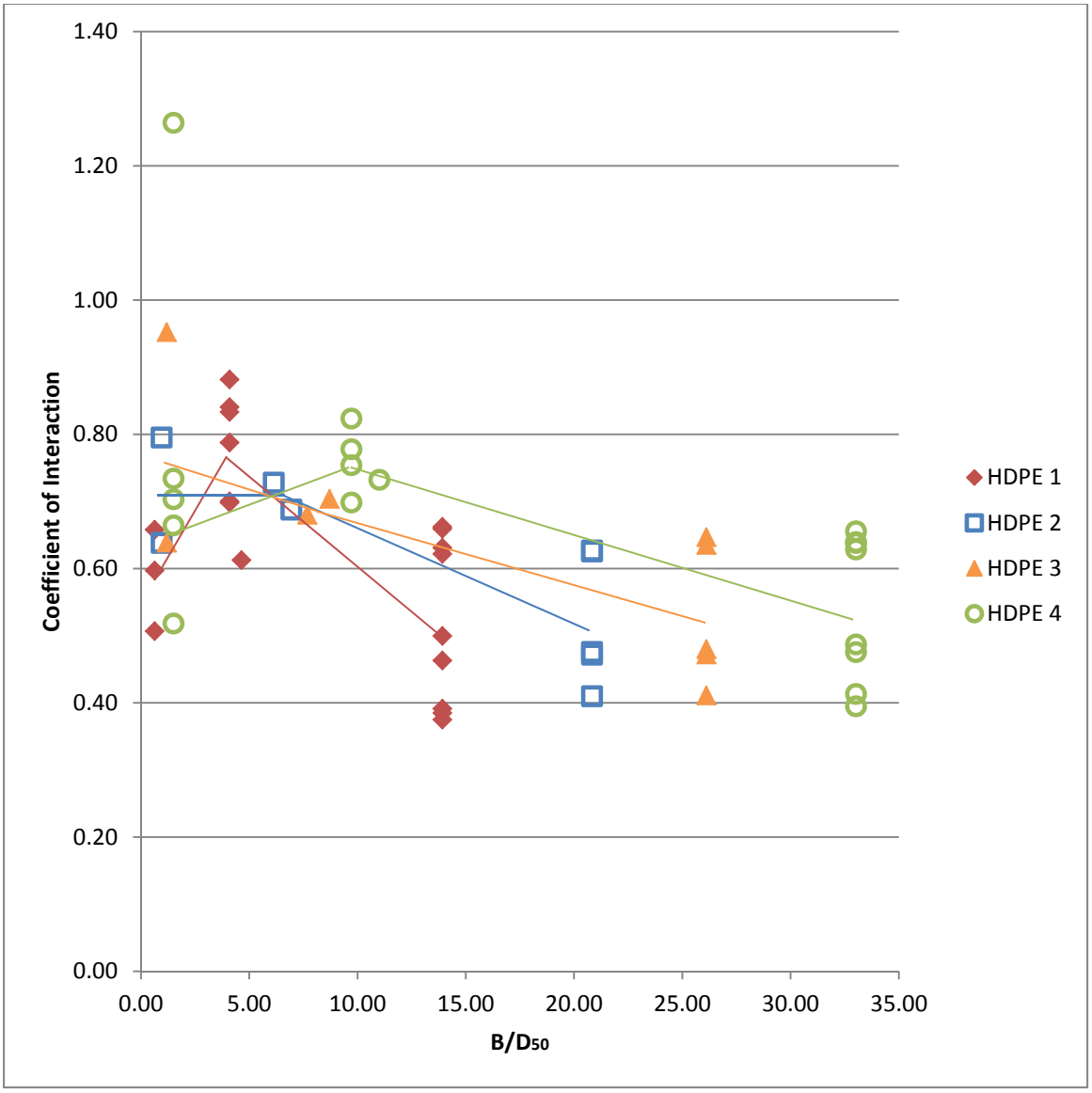

Figure 5.11 Influence of the ratio transverse rib thickness to mean particle diameter on coefficient of interaction, by specific geogrid.

Chapter 6: Summary and Conclusions

6.1 SUMMARY

Determining the coefficient of interaction between a geogrid and a particular fill material requires conducting pullout tests, one of the most expensive geotechnical laboratory tests. The pullout test used to determine the CI is a very time consuming process, requiring up to two days to perform a single test. The CI value is needed to determine the proper spacing and embedment length of the reinforcement in a MSE wall design. This thesis presents a summary of results for a large number of pullout tests, performed on many geogrid/fill material combinations, so that CI values may be interpolated for preliminary design. Test results are presented in tabular and graphic form in Appendix A. An important note is that all test results presented in this thesis were performed by a single laboratory, therefore errors due to differing laboratory equipment and testing procedures are minimized. All tests were performed according to what is now ASTM D 6706-01 "Standard Test Method for Measuring Geosynthetic Pullout Resistance in Soil."

The CI values in the database range from 0.38 to 1.52. The geogrid/fill material combination that correspond with this minimum and this maximum are HDPE1 in Silty Sand and PET 1 in Gravel 1, respectively. These combinations come as no surprise to represent the extreme values. Geogrids tested in Silty Sand consistently produced CI values well below all other fill materials, and the HDPE geogrids had poorer results (lower CI for a given normal stress) in the Silty Sand the PET geogrids. On the other end of the spectrum, well graded fill materials (including Gravel 1) showed increasing trends in CI with increasing normal stress. PET 1 has an ultimate tensile strength of 9,500 lbs/ft, so a very large normal pressure could be used during testing of the product. Since the

well graded materials showed a proportional relationship between CI and normal stress, a large CI was likely with the PET 1 product.

This thesis analyzes the following: the effects of geogrid polymer type on CI; the effects of the presence of fines on CI; the effects of specimen embedment length on CI and bearing stress; and the effects of B/D_{50} on bearing stress.

6.2 CONCLUSIONS

6.2.1 Effects of Geogrid Polymer Type

Tests reviewed in this study were conducted on uniaxial geogrids made of either HDPE or PET. The two grids materials exhibit similar trends in pullout data when tested in the same fill material. Both geogrid materials exhibited CI values that remained constant with increasing normal stress when tested in Silty Sand, and an increasing trend when tested in Gravel 2. An exception was noted for tests performed in the Sand 1 (poorly graded sand) fill material, where the PET geogrid showed a constant CI value with increasing normal stress and the HDPE geogrid showed a decreasing CI trend with increasing normal stress.

6.2.2 Effects of the Presences of Fines

The presences of a significant percentage of fines in the fill material were analyzed for both PET and HDPE geogrids. A significant percentage was defined as greater than 12% for this study. For both polymer types, a reduction in CI value is shown when fines are present. There was a greater reduction in CI value for soils with silty fines than with clayey fines. HDPE geogrids show relatively constant CI values across the range of normal stresses tested when fines are present. PET geogrids show a positive CI rate of change with increasing normal stress when fines are present.

6.2.3 Effects of Geogrid Embedment Length

HDPE geogrids show sensitivity to embedment length during testing. While specimens with greater length produce greater pullout resistance, the actual load per unit area carried by the geogrid is greater in shorter length specimens. The series of test with shorter samples (40 inches) exhibit a greater rate of change, with respect to CI value, than do longer samples (70 inches). The effects of embedment length are also apparent when analyzing normalized bearing stress. Here the shorter samples show a decreasing trend in normalized bearing stress with increasing B/D_{50} to a point, then the normalized bearing stress remains constant with increasing B/D_{50} from then on after. The longer samples show a decreasing trend in normalized bearing stress over the full range of B/D_{50} tested.

6.2.4 Effects of B/D_{50} on Normalized Bearing Stress

The data were analyzed to identify how the B/D_{50} ratio effects normalized bearing stress. When the data are organized by fill material, the trends show a linear decrease in normalized bearing stress with increasing B/D_{50}. Except for the series of tests performed with shorter samples (40 inches), the decreasing trend persisted across the full range of B/D_{50} values tested.

Organizing the results by geogrid suggests that bearing stress increases for B/D_{50} values from zero to between 5 and 10. A peak in normalized bearing stress is reached in this range, and then a decreasing trend continues from that point on after for increasing values of B/D_{50}. Plotting CI against B/D_{50}, grouped by geogrid, results in trends very similar to the trends identified for normalized bearing stress versus B/D_{50}.

6.3 RECOMMENDATIONS

Recommendations were developed as a result of the database analysis. These recommendations are related to data collected during geogrid testing and better understanding of the effect of geogrid specimen length on pullout resistance results.

In regards to laboratory geogrid testing, it would be useful to have a standard set of data that should be included with each testing results report. These would include: geogrid polymer type, whether it is uniaxial or biaxial, specific dimensions of the product (rib width, thickness and spacing), fill material total and effective strength, and the gradation of the fill material. These additional reported values could greatly benefit the profession as a whole by allowing better correlation to be developed, and with possibly developing a better understanding of the interactions occurring between the geogrid and fill material.

In regards to the effects of geogrid specimen length on pullout results, additional research could be conducted to evaluate how to accurately apply the measured interaction values from laboratory testing to the actual design for field use. Past studies have verified that the effects of specimen length begin to diminish with increasing lengths. It would be used full to know how long a particular geogrid specimen would need to be in order to produce results that are fairly representative of field conditions. It would also be useful to develop a conversion equation that could adjust the results from shorter samples so that they are in better agreement with field values. Testing of shorter samples requires much less time, materials and expenses.

Appendix A: Summary of Pullout Testing Database

Table A.1 Summary of Database Test Results.

Geogrid ID	Soil ID	Embedded		Normal Stress (psi)	Pullout Resistance (lbs/ft)	CI
		Length (in)	Width (in)			
HDPE 1	Clayey Sand	70.0	18.0	2.0	2592	0.63
HDPE 1	Clayey Sand	70.0	18.0	2.0	2708	0.66
HDPE 1	Clayey Sand	70.0	18.0	4.0	3911	0.62
HDPE 1	Clayey Sand	70.0	18.0	4.0	4165	0.66
HDPE 1	Gravel 2	40.0	18.0	2.4	2147	0.66
HDPE 1	Gravel 2	70.0	18.0	2.0	2673	0.51
HDPE 1	Gravel 2	70.0	18.0	4.0	4453	0.60
HDPE 1	Sand 1	70.0	18.0	2.0	2798	0.88
HDPE 1	Sand 1	70.0	18.0	2.0	2668	0.84
HDPE 1	Sand 1	70.0	18.0	2.0	2216	0.70
HDPE 1	Sand 1	70.0	18.0	4.0	4755	0.83
HDPE 1	Sand 1	70.0	18.0	4.0	4495	0.79
HDPE 1	Sand 1	70.0	18.0	4.0	3995	0.70
HDPE 1	Sand 7	38.0	18.0	2.4	1600	0.61
HDPE 1	Silty Sand	70.0	18.0	2.0	1914	0.46
HDPE 1	Silty Sand	70.0	18.0	2.0	1591	0.38
HDPE 1	Silty Sand	70.0	18.0	4.0	3197	0.50
HDPE 1	Silty Sand	70.0	18.0	4.0	2400	0.38
HDPE 1	Unknown 3	70.0	18.0	2.5	2427	0.39
HDPE 2	Clayey Sand	70.0	18.0	2.0	2575	0.63
HDPE 2	Clayey Sand	70.0	18.0	8.0	6665	0.63
HDPE 2	Gravel 2	40.0	18.0	4.4	3587	0.80
HDPE 2	Gravel 2	70.0	18.0	4.0	4760	0.64
HDPE 2	Sand 1	70.0	18.0	4.0	4154	0.73
HDPE 2	Sand 7	38.0	18.0	4.4	2967	0.69
HDPE 2	Silty Sand	70.0	18.0	2.0	1967	0.48
HDPE 2	Silty Sand	70.0	18.0	4.0	2623	0.41
HDPE 2	Silty Sand	70.0	18.0	8.0	5159	0.47
HDPE 2	Unknown 1	72.5	18.0	4.0	2940	0.53
HDPE 2	Unknown 1	73.0	18.0	8.0	4109	0.43
HDPE 2	Unknown 2	71.5	18.0	8.0	3818	0.40

Geogrid ID	Soil ID	Embedded		Normal Stress (psi)	Pullout Resistance (lbs/ft)	CI
		Length (in)	Width (in)			
HDPE 3	Clayey Sand	70.0	18.0	2.0	2657	0.65
HDPE 3	Clayey Sand	70.0	18.0	8.0	6767	0.64
HDPE 3	Gravel 2	40.0	18.0	5.9	5186	0.95
HDPE 3	Gravel 2	70.0	18.0	6.0	6156	0.64
HDPE 3	Sand 1	70.0	18.0	6.0	5603	0.68
HDPE 3	Sand 5	47.0	18.5	7.0	4242	0.94
HDPE 3	Sand 6	50.8	18.5	1.3	1356	0.88
HDPE 3	Sand 6	50.8	18.5	4.5	2836	0.65
HDPE 3	Sand 6	50.8	18.5	9.0	5521	0.66
HDPE 3	Sand 7	38.0	18.0	5.9	3933	0.70
HDPE 3	Silty Sand	70.0	18.0	2.0	1985	0.48
HDPE 3	Silty Sand	70.0	18.0	6.0	3562	0.41
HDPE 3	Silty Sand	70.0	18.0	8.0	5161	0.47
HDPE 4	Clayey Sand	70.0	18.0	2.0	2621	0.64
HDPE 4	Clayey Sand	70.0	18.0	2.0	2693	0.66
HDPE 4	Clayey Sand	70.0	18.0	8.0	6813	0.64
HDPE 4	Clayey Sand	70.0	18.0	8.0	6697	0.63
HDPE 4	Gravel 2	40.0	18.0	7.4	8066	1.26
HDPE 4	Gravel 2	70.0	18.0	2.0	2733	0.52
HDPE 4	Gravel 2	70.0	18.0	4.0	4954	0.66
HDPE 4	Gravel 2	70.0	18.0	8.0	8679	0.73
HDPE 4	Gravel 2	70.0	18.0	8.0	8314	0.70
HDPE 4	Sand 1	70.0	18.0	2.0	2614	0.82
HDPE 4	Sand 1	70.0	18.0	4.0	4303	0.75
HDPE 4	Sand 1	70.0	18.0	8.0	8379	0.78
HDPE 4	Sand 1	70.0	18.0	8.0	7523	0.70
HDPE 4	Sand 2	49.0	18.0	15.0	9533	0.80
HDPE 4	Sand 7	38.0	18.0	7.4	5027	0.73
HDPE 4	Silty Sand	70.0	18.0	2.0	2013	0.49
HDPE 4	Silty Sand	70.0	18.0	4.0	2527	0.39
HDPE 4	Silty Sand	70.0	18.0	8.0	5200	0.48

Geogrid ID	Soil ID	Embedded		Normal Stress (psi)	Pullout Resistance (lbs/ft)	CI
		Length (in)	Width (in)			
HDPE 4	Silty Sand	70.0	18.0	8.0	4519	0.41
PET 1	Clay	36.0	18.0	8.0	5399	0.79
PET 1	Clay	36.5	18.0	4.0	3065	0.79
PET 1	Gravel 1	36.0	18.5	4.7	4177	1.52
PET 1	Sand 1	36.0	18.0	3.0	1973	0.86
PET 1	Sand 1	36.0	18.0	6.0	3587	0.85
PET 1	Sand 1	36.0	18.0	12.0	6591	0.81
PET 1	Sand 5	48.0	18.0	7.0	4432	0.96
PET 10	Sand 2	47.0	15.0	3.5	2483	1.05
PET 10	Sand 2	47.0	15.0	7.0	4772	1.03
PET 10	Sand 5	48.0	17.5	5.0	3325	0.98
PET 10	Sand 5	48.0	17.5	7.0	4573	0.99
PET 10	Sand 5	48.0	18.0	10.0	5786	0.90
PET 2	Sand 1	36.0	18.0	1.0	791	0.81
PET 2	Sand 1	36.0	18.0	2.0	1268	0.78
PET 2	Sand 1	36.0	18.0	4.0	2371	0.81
PET 3	Clay	36.0	18.0	2.0	1888	0.81
PET 3	Clay	36.5	18.0	1.0	1221	0.76
PET 3	Sand 1	36.0	18.0	1.0	799	0.81
PET 3	Sand 1	36.0	18.0	2.0	1331	0.82
PET 3	Sand 1	36.0	18.0	4.0	2378	0.81
PET 4	Sand 1	36.0	18.0	1.0	798	0.81
PET 4	Sand 1	36.0	18.0	3.0	1890	0.83
PET 4	Sand 1	36.0	18.0	6.0	3463	0.82
PET 5	Sand 1	36.0	18.0	2.0	1333	0.82
PET 5	Sand 1	36.0	18.0	4.0	2423	0.83
PET 5	Sand 1	36.0	18.0	8.0	4525	0.82
PET 6	Sand 1	48.0	14.0	2.5	2317	0.89
PET 7	Gravel 2	48.0	18.0	2.0	1752	0.48
PET 7	Gravel 2	48.0	18.0	4.0	3270	0.64
PET 7	Silty Sand	48.0	18.0	2.0	2010	0.71

Geogrid ID	Soil ID	Embedded		Normal Stress (psi)	Pullout Resistance (lbs/ft)	CI
		Length (in)	Width (in)			
PET 7	Silty Sand	48.0	18.0	4.0	3145	0.72
PET 7	Silty Sand	48.0	18.0	8.0	5207	0.69
PET 8	Sand 2	46.0	14.8	3.5	2566	1.11
PET 8	Sand 2	46.0	14.8	7.0	4438	0.98
PET 8	Sand 2	46.0	14.8	14.0	9192	1.02
PET 9	Sand 2	48.5	14.5	3.5	3193	1.31
PET 9	Sand 2	48.5	14.5	7.0	5094	1.06
PET 9	Sand 2	48.5	14.5	14.0	9880	1.04

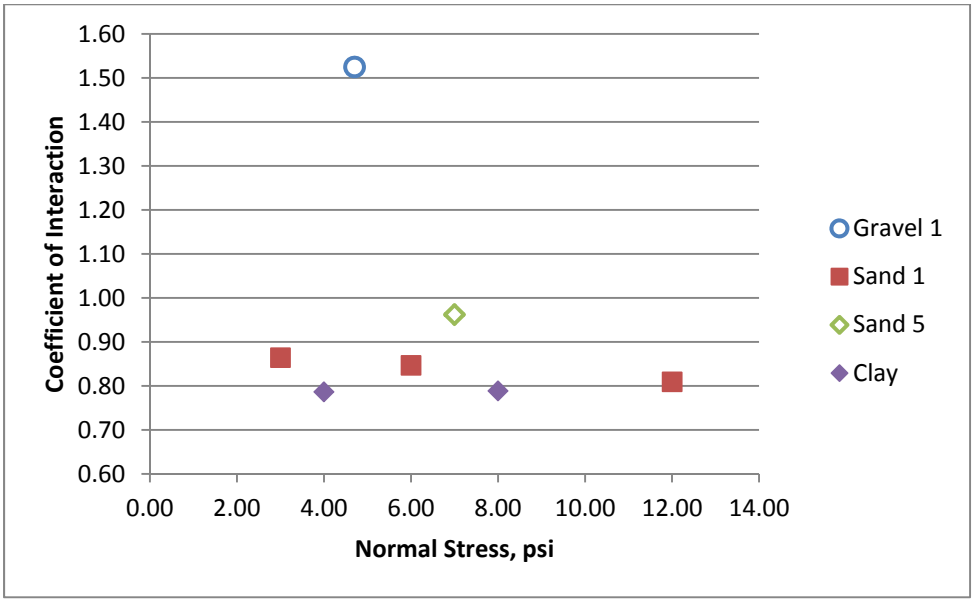

Figure A.1: Geogrid PET 1 tested in various fill materials.

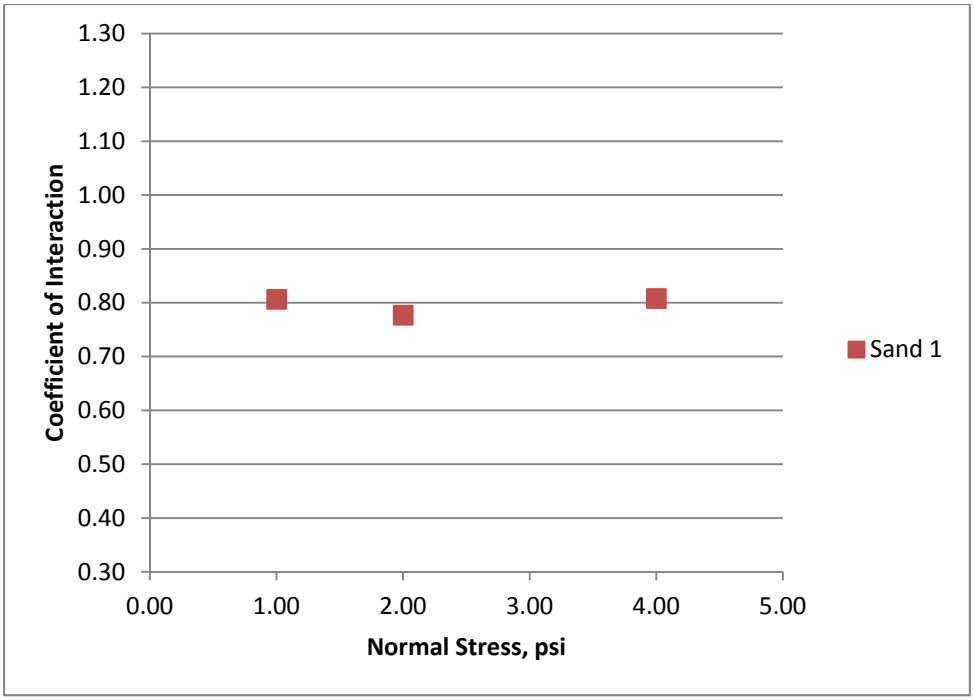

Figure A.2: Geogrid PET 2 tested in Sand 1 fill material.

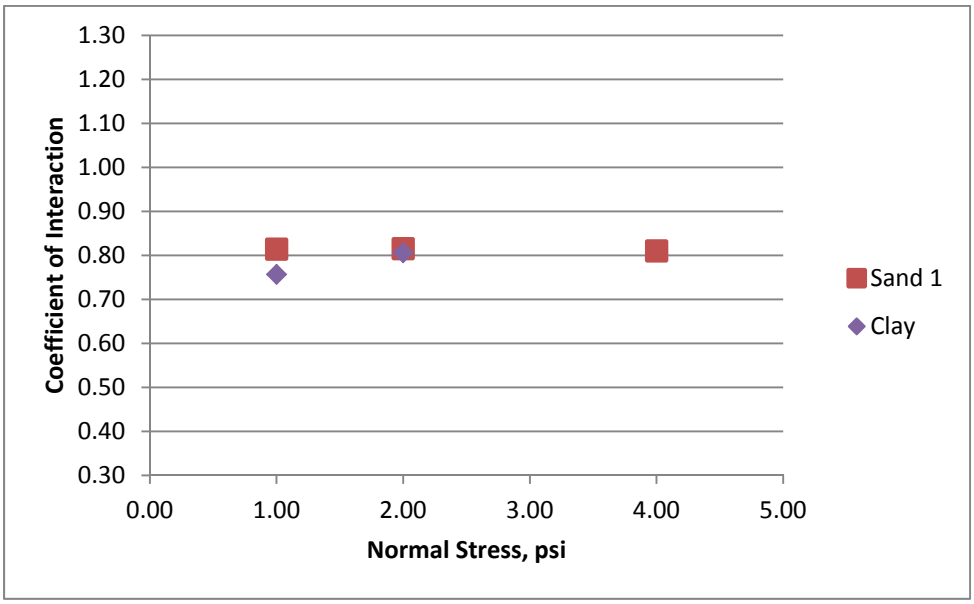

Figure A.3: Geogrid PET 3 tested in various fill materials.

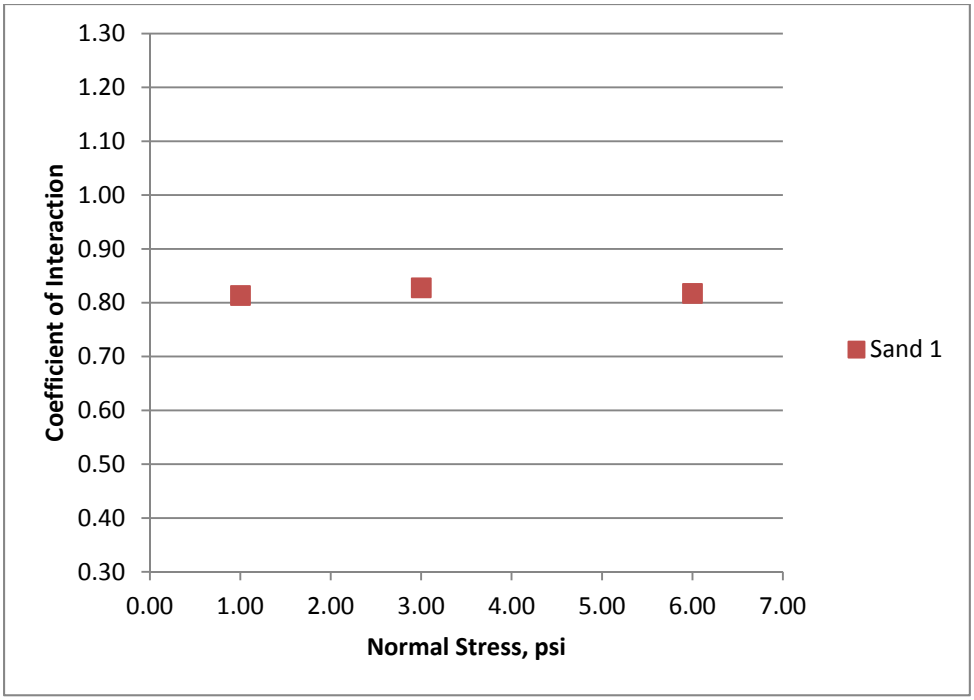

Figure A.4: Geogrid PET 4 tested in Sand 1 fill material.

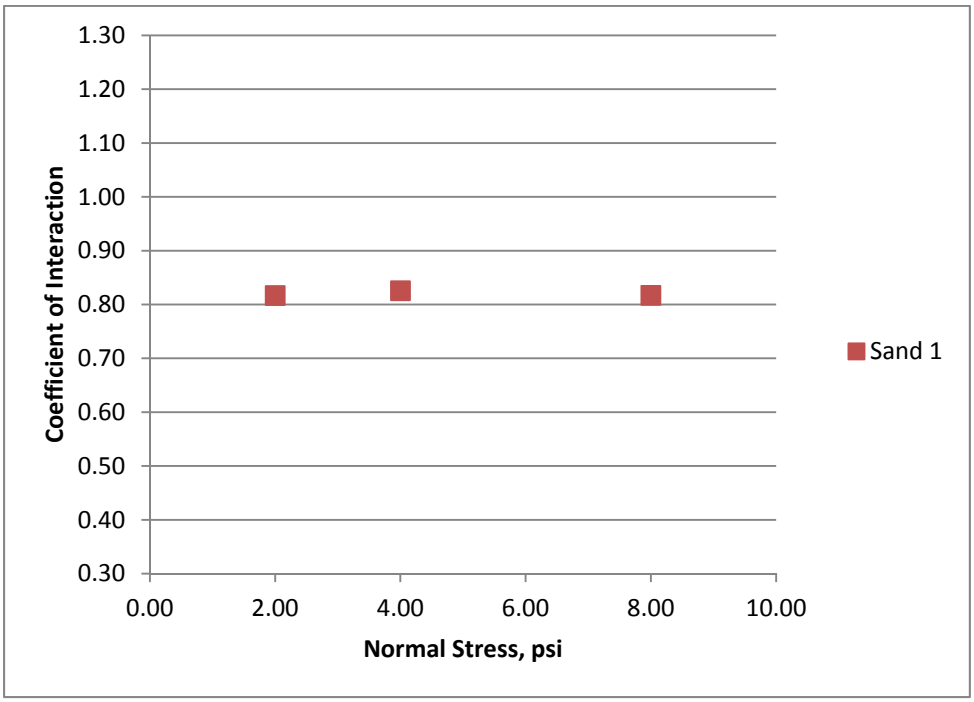

Figure A.5: Geogrid PET 5 tested in Sand 1 fill material.

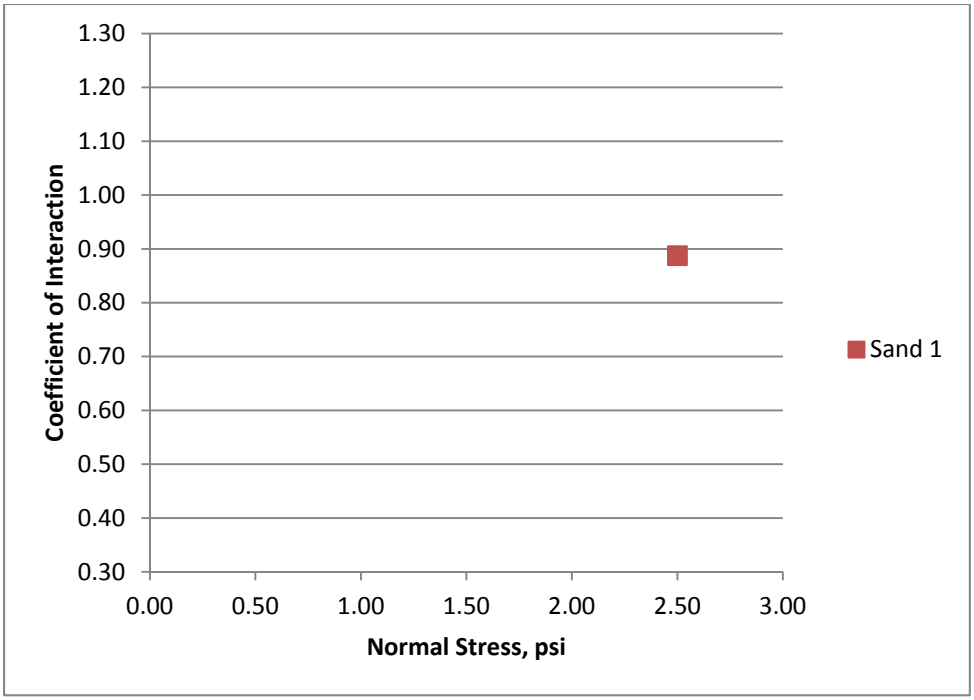

Figure A.6: Geogrid PET 6 tested in Sand 1 fill material.

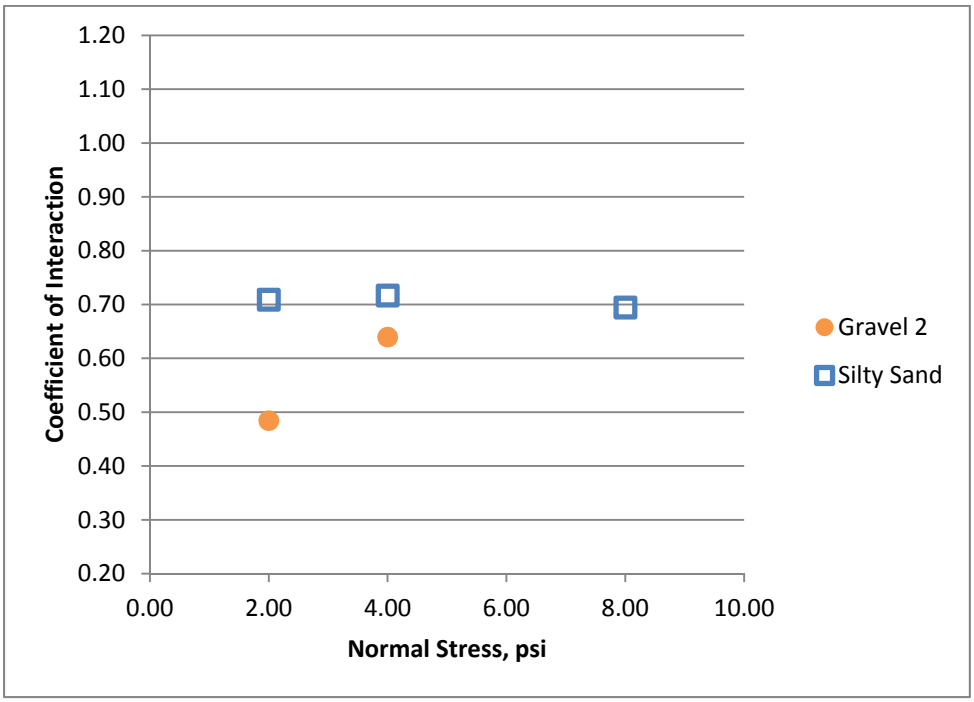

Figure A.7: Geogrid PET 7 tested in various fill materials.

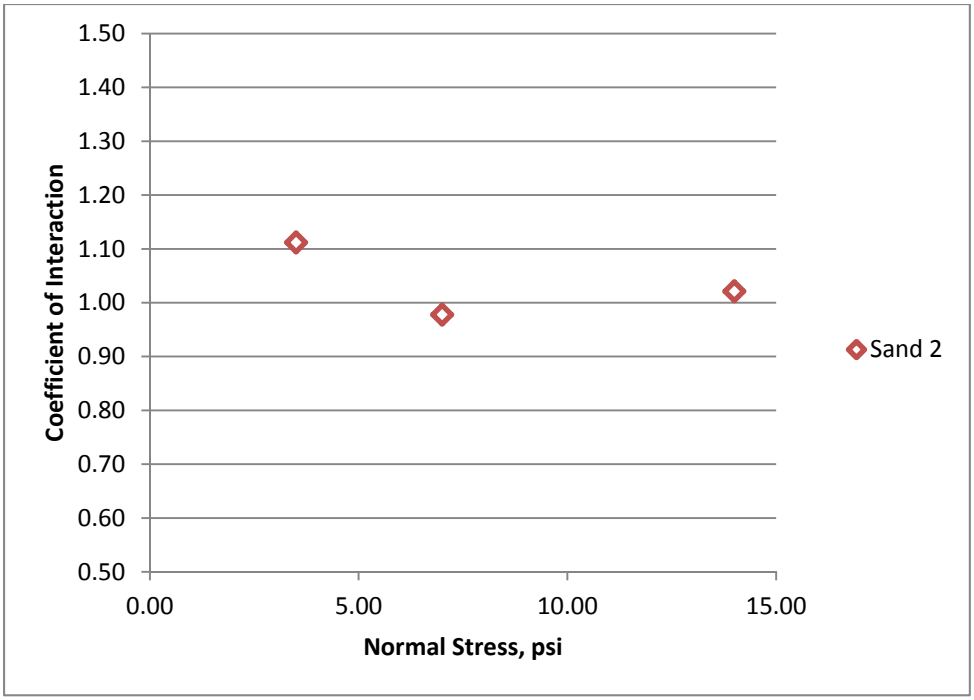

Figure A.8: Geogrid PET 8 tested in Sand 2 fill material.

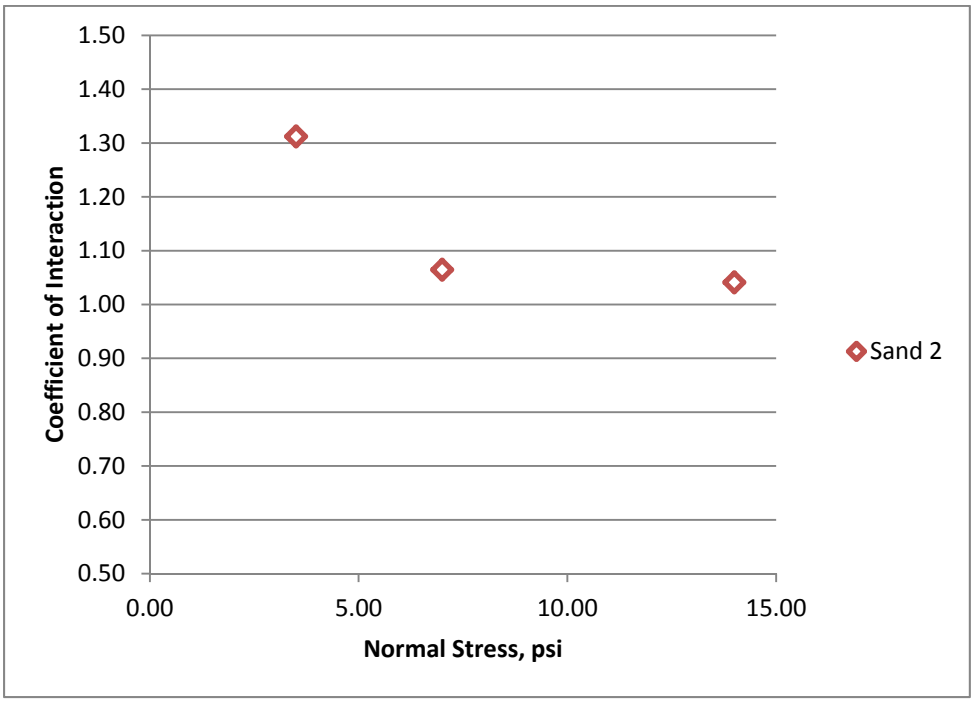

Figure A.9: Geogrid PET 9 tested in Sand 2 fill material.

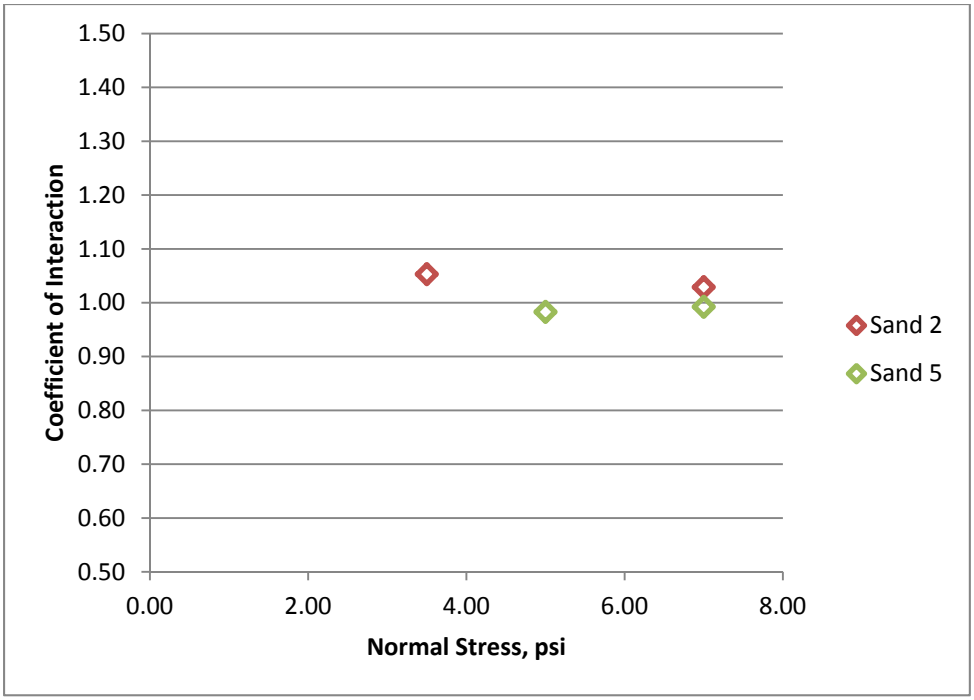

Figure A.10: Geogrid PET 10 tested in various fill materials.

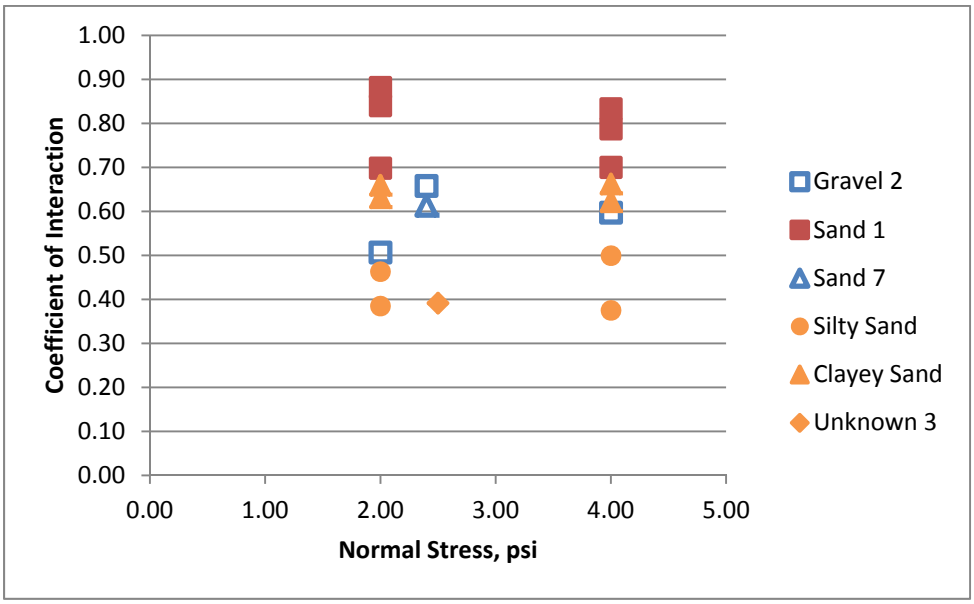

Figure A.11: Geogrid HDPE 1 tested in various fill materials.

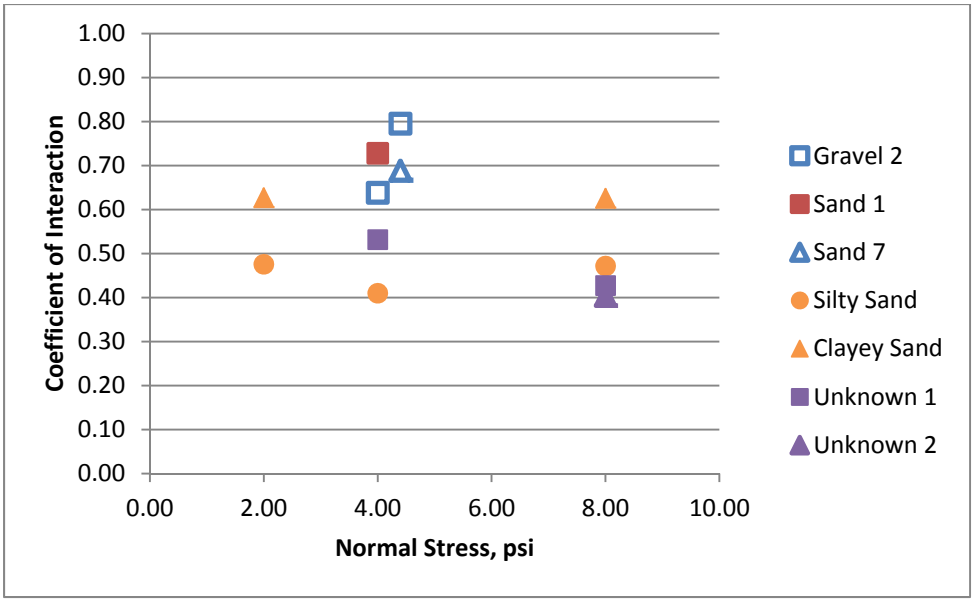

Figure A.12: Geogrid HDPE 2 tested in various fill materials.

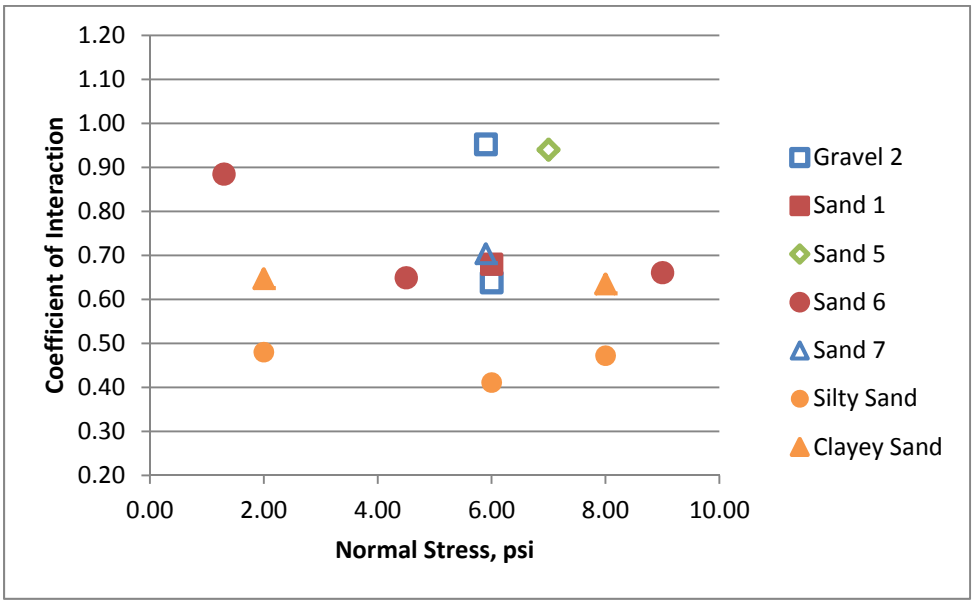

Figure A.13: Geogrid HDPE 3 tested in various fill materials.

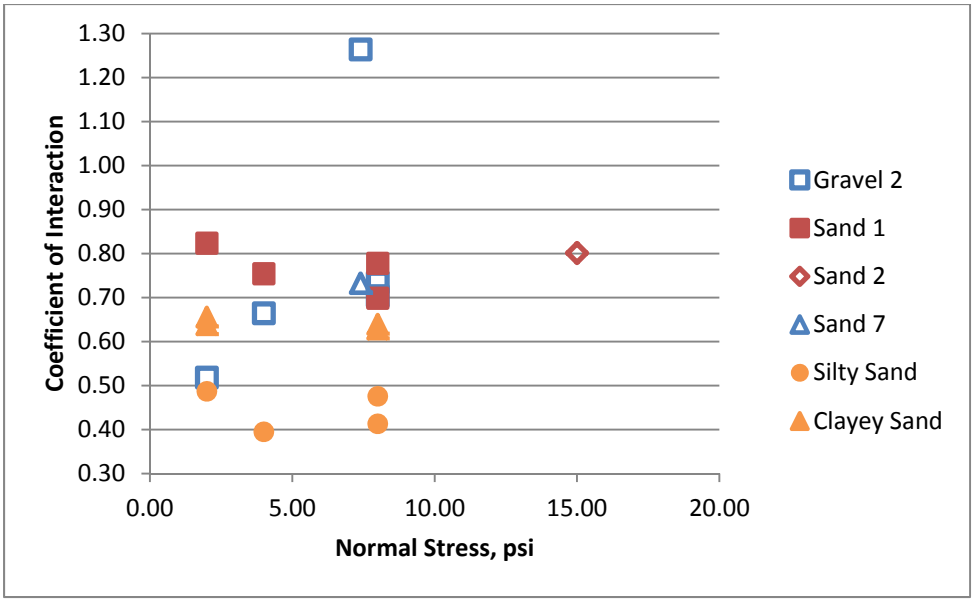

Figure A.14: Geogrid HDPE 4 tested in various fill materials.

Appendix B: Fill Material Gradation and Compaction Information

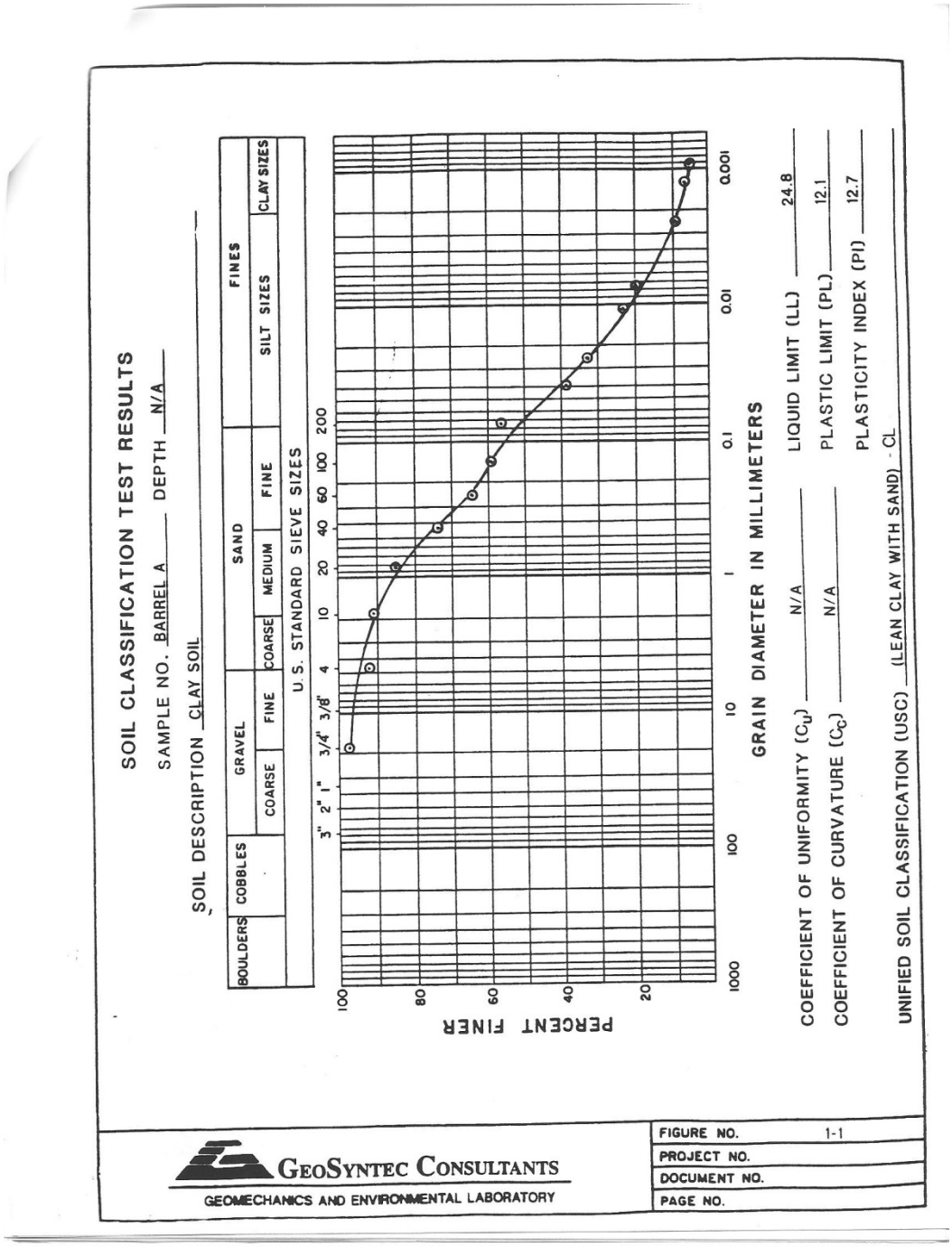

Figure B.1: Gradation report for Clay fill material.

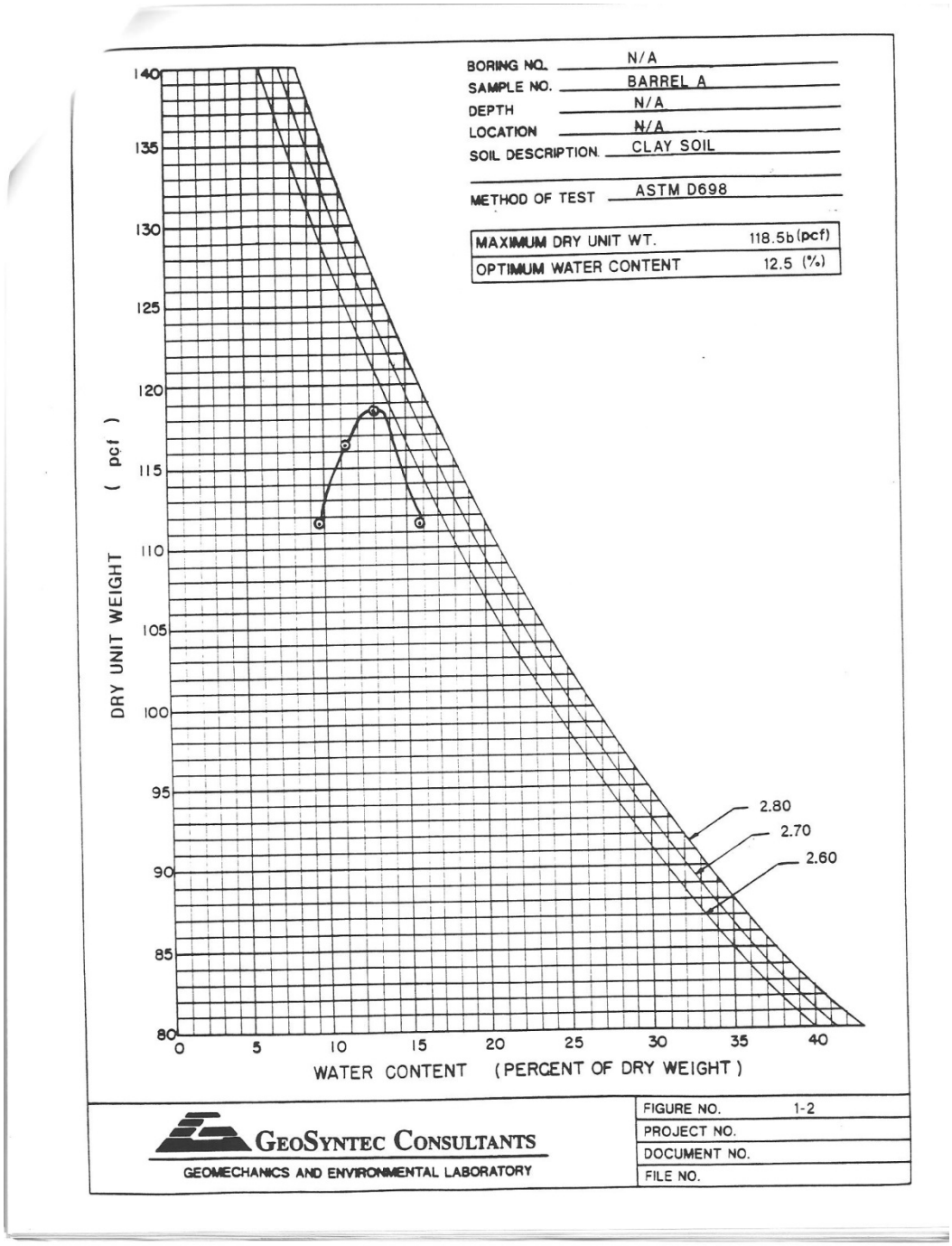

Figure B.2: Compaction report for Clay fill material.

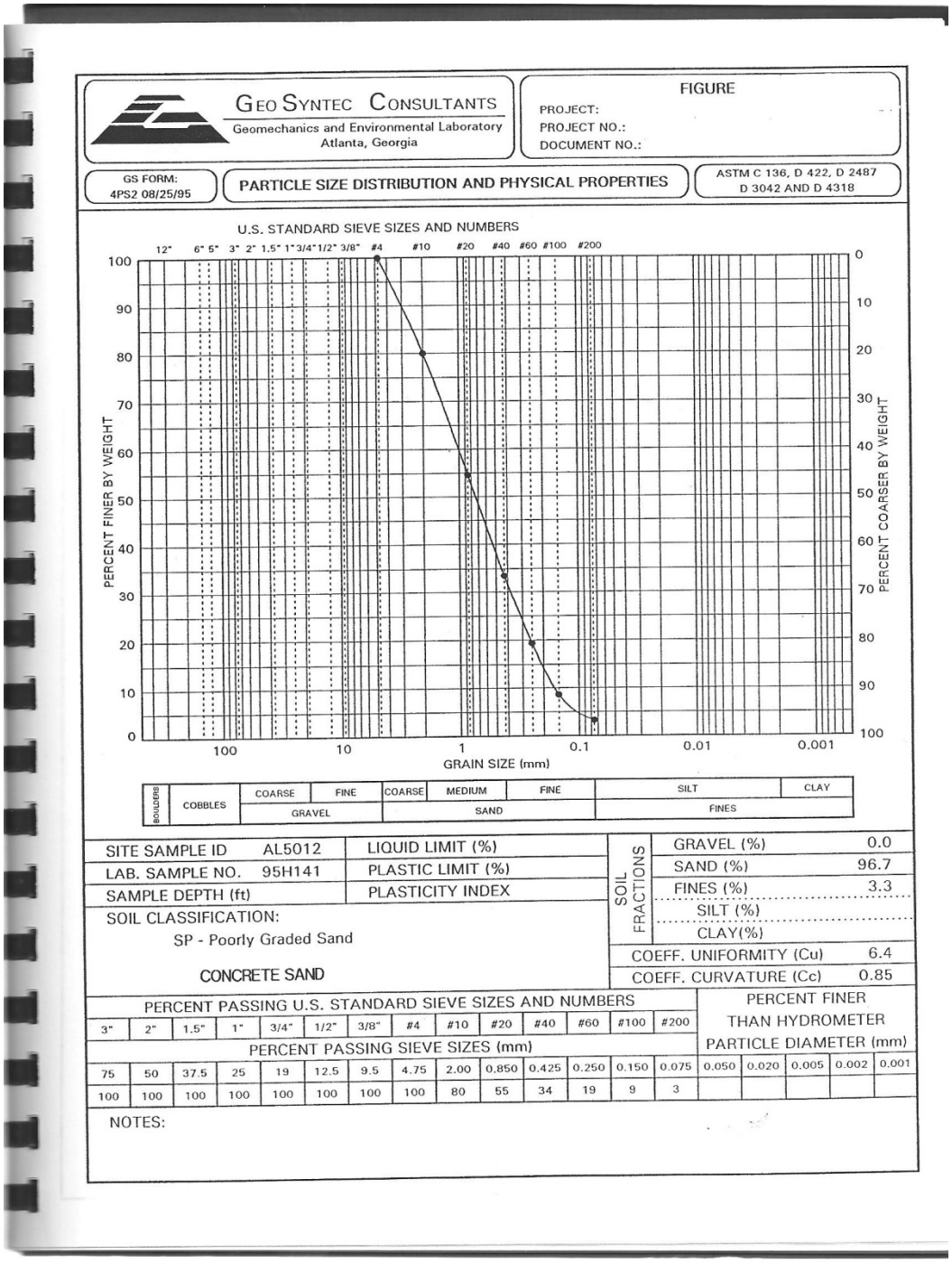

Figure B.3: Gradation report for Sand 1 fill material.

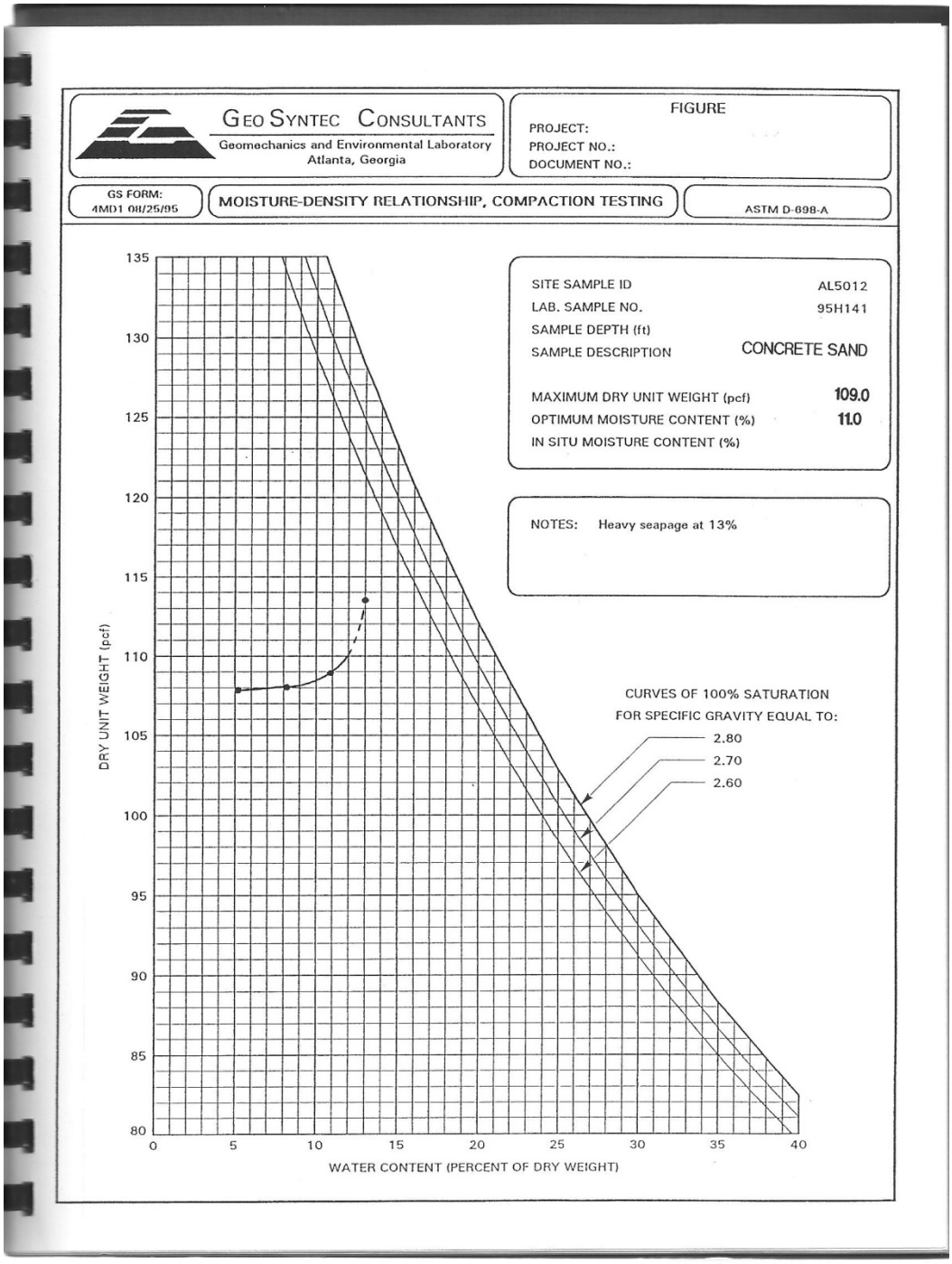

Figure B.4: Compaction report for Sand 1 fill material.

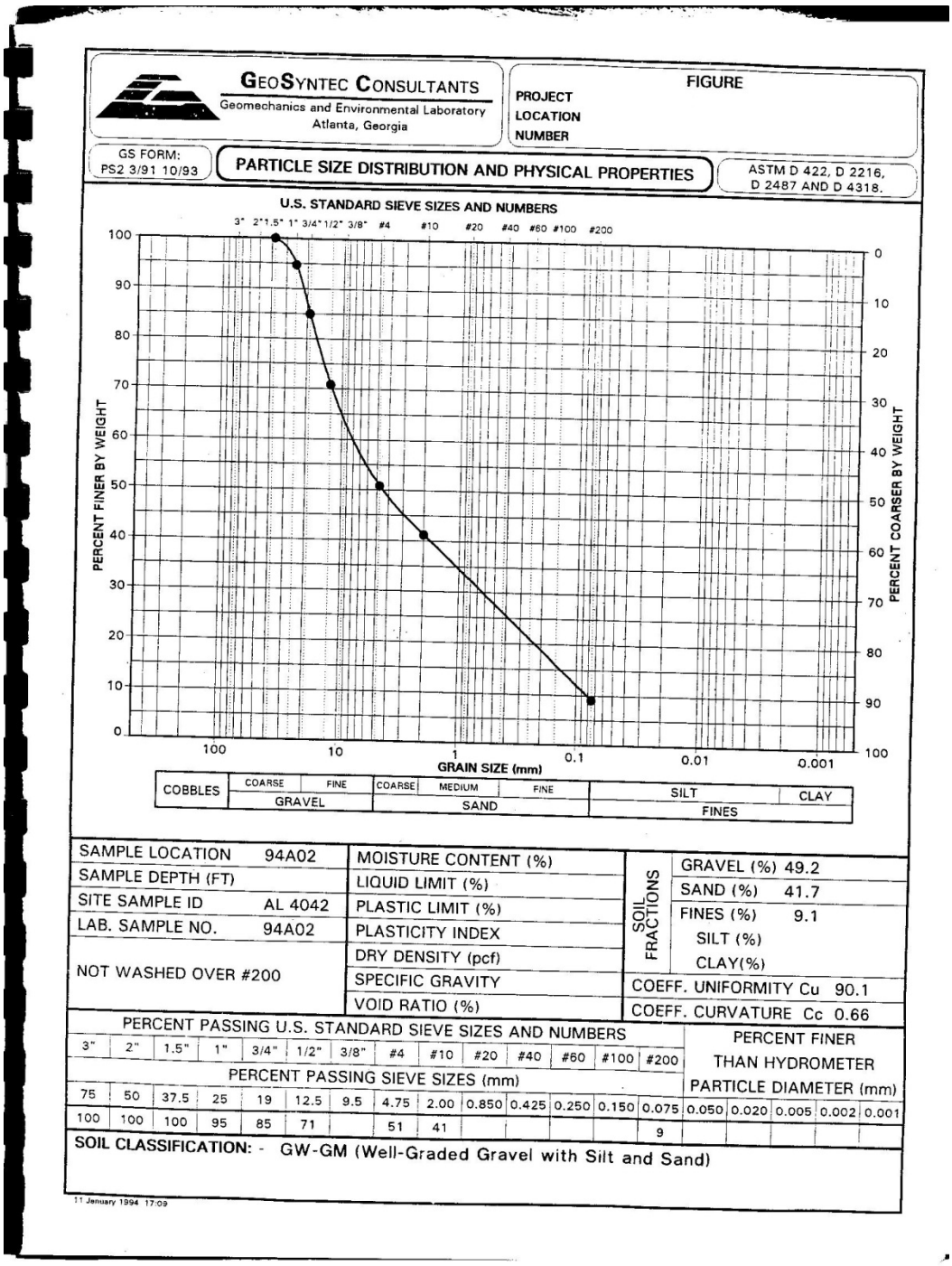

Figure B.5: Gradation report for Gravel 1 fill material.

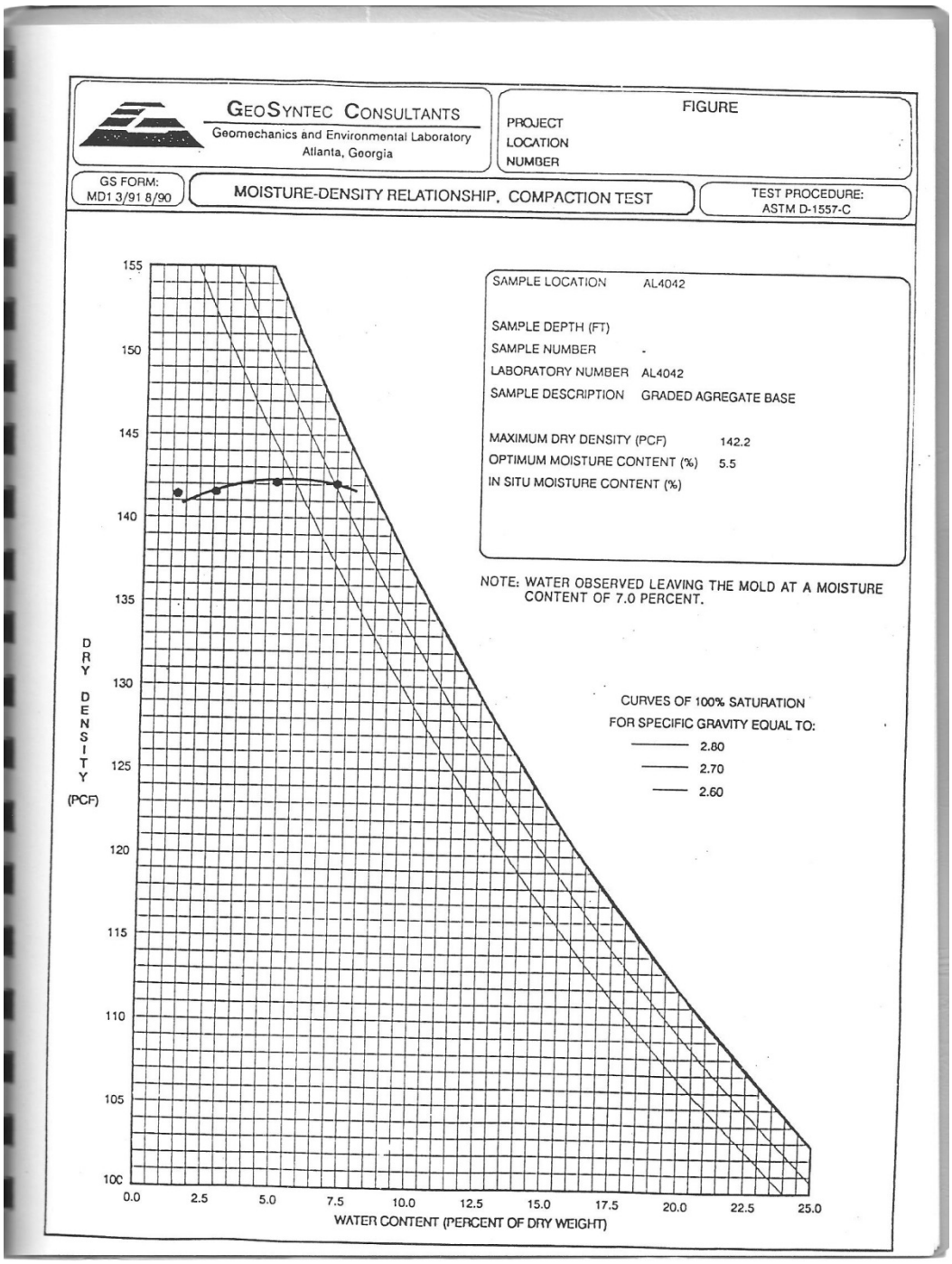

Figure B.6: Compaction report for Gravel 1 fill material.

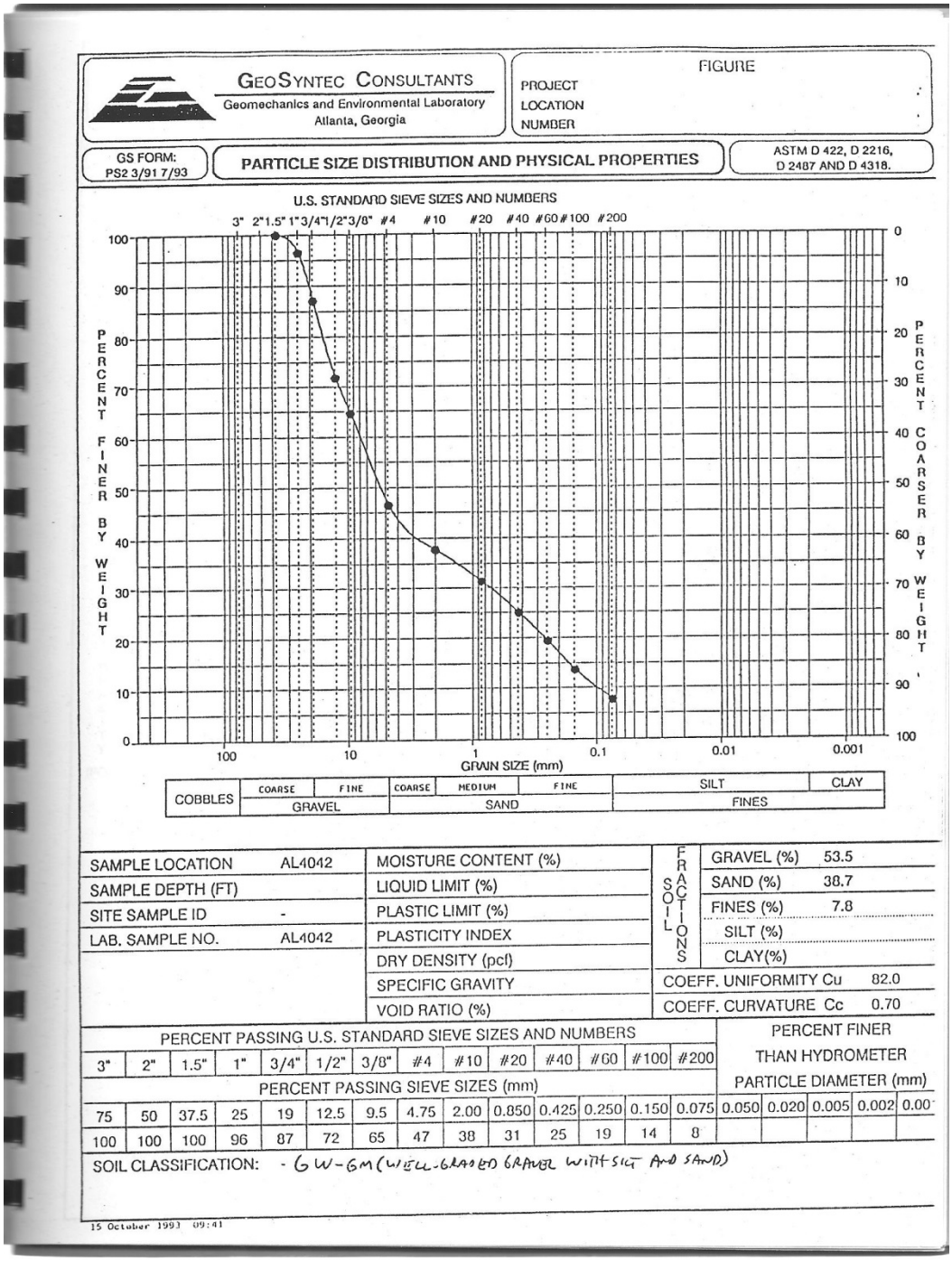

Figure B.7: Gradation report for Gravel 2 fill material.

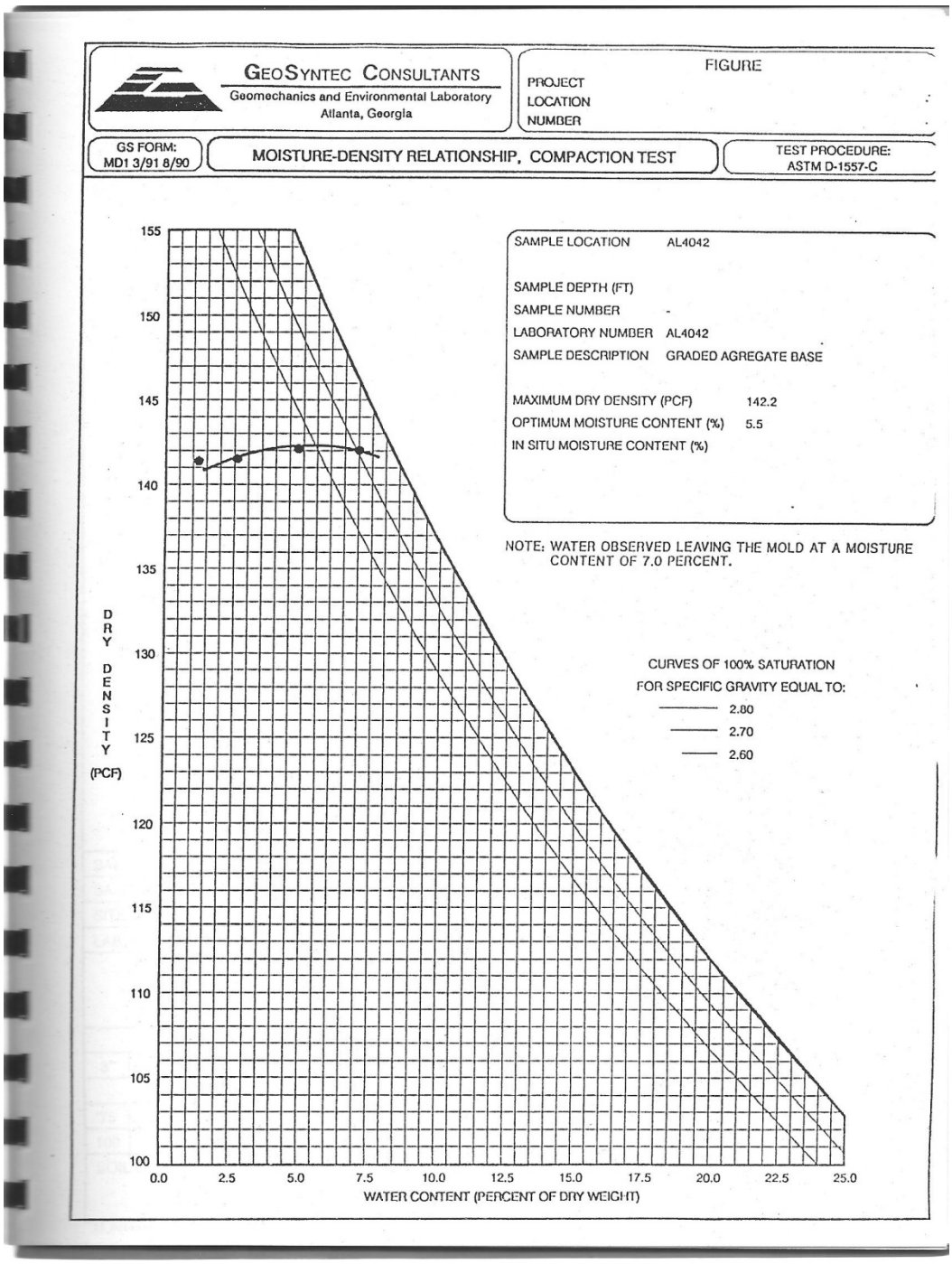

Figure B.8: Compaction report for Gravel 2 fill material.

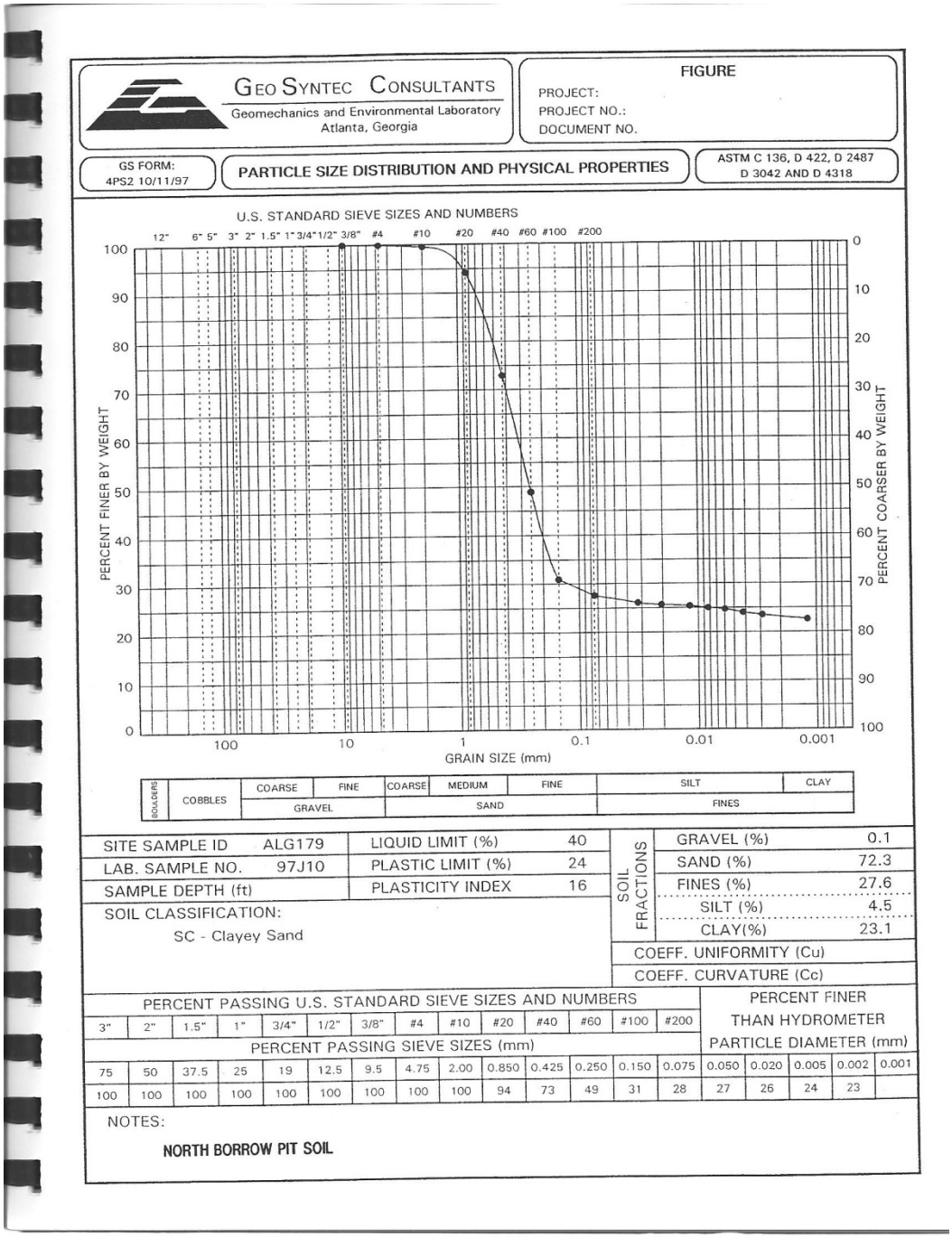

Figure B.9: Gradation report for Clayey Sand fill material.

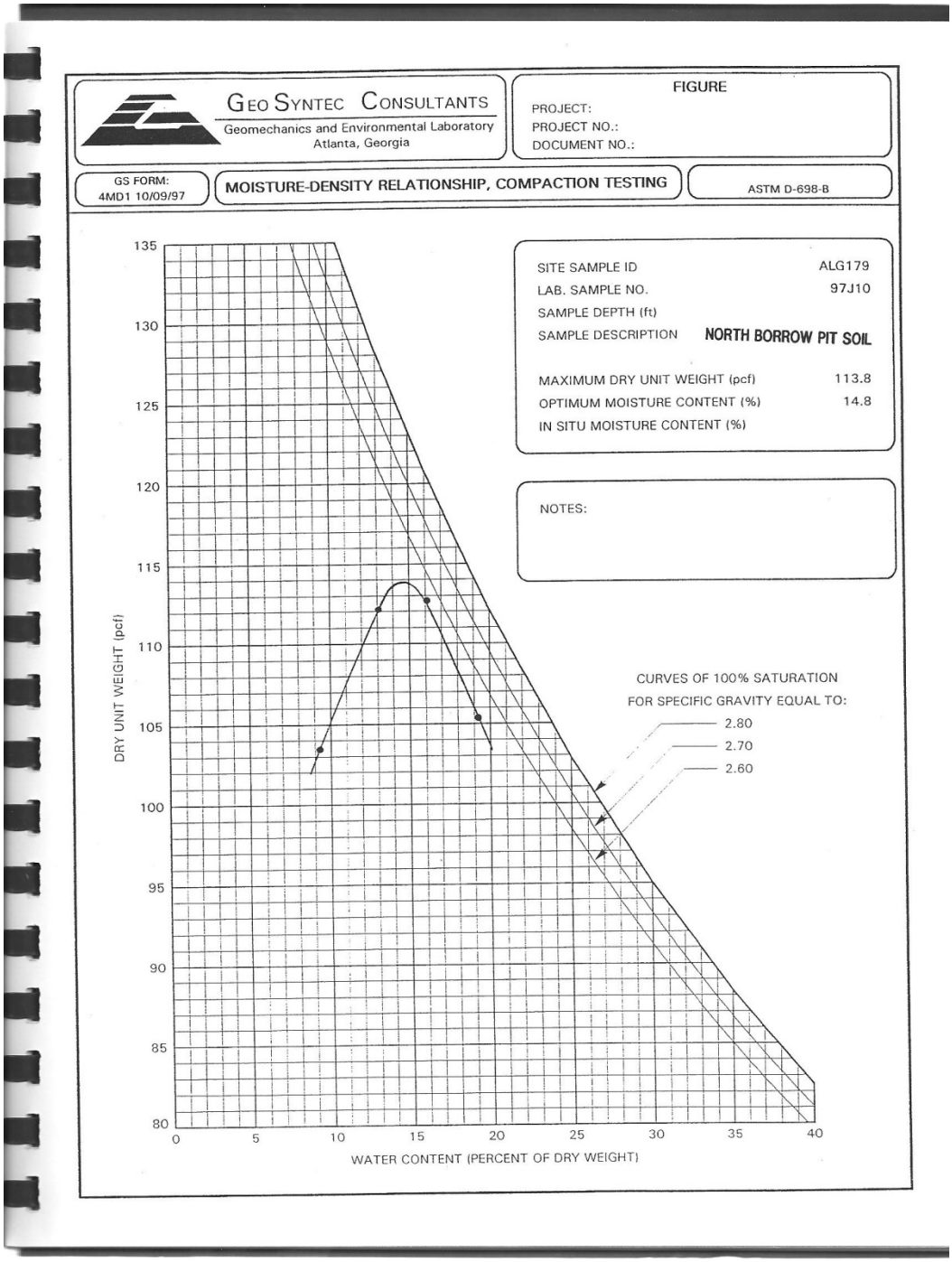

Figure B.10: Compaction report for Clayey Sand fill material.

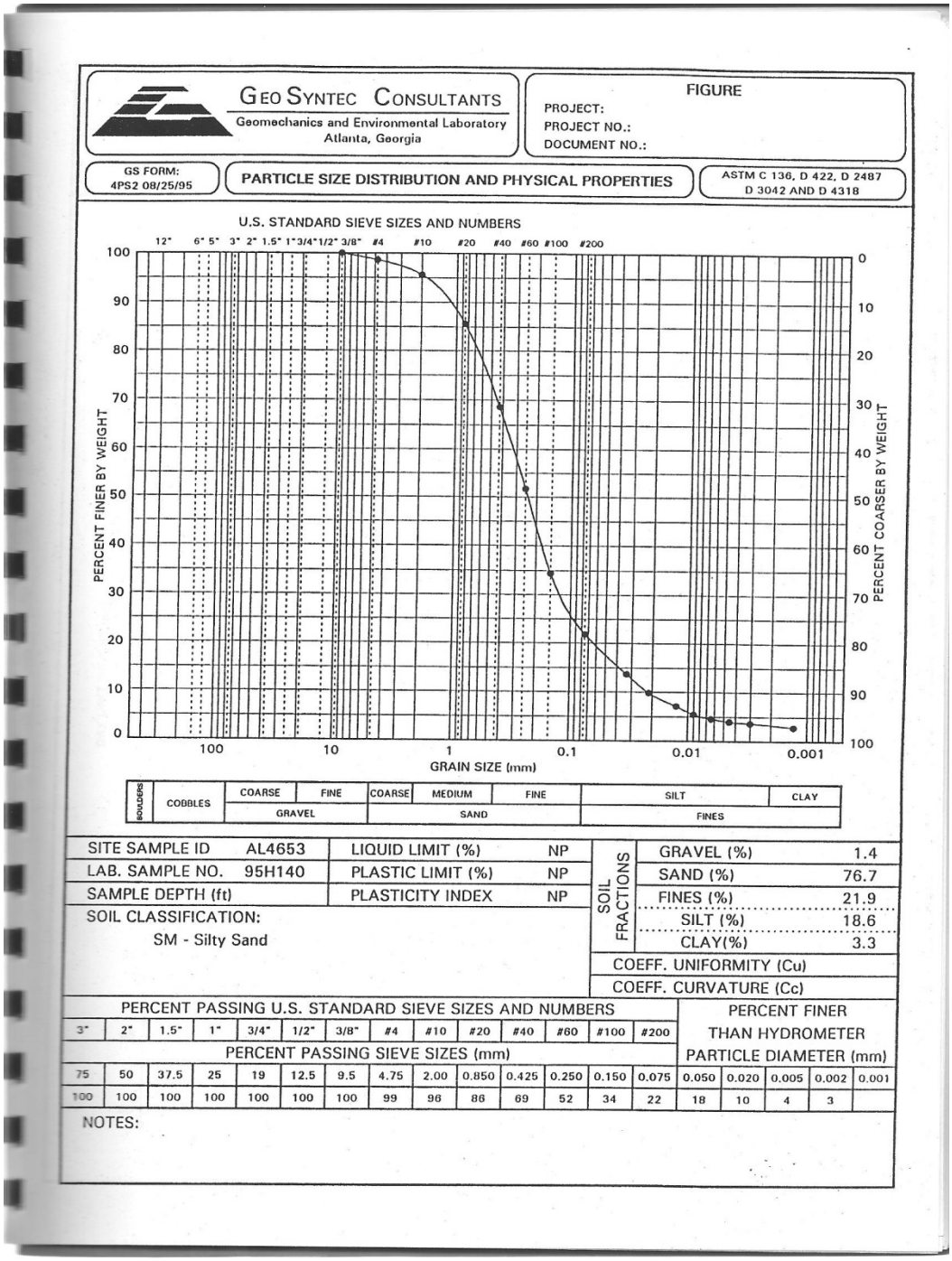

Figure B.11: Gradation report for Silty Sand fill material.

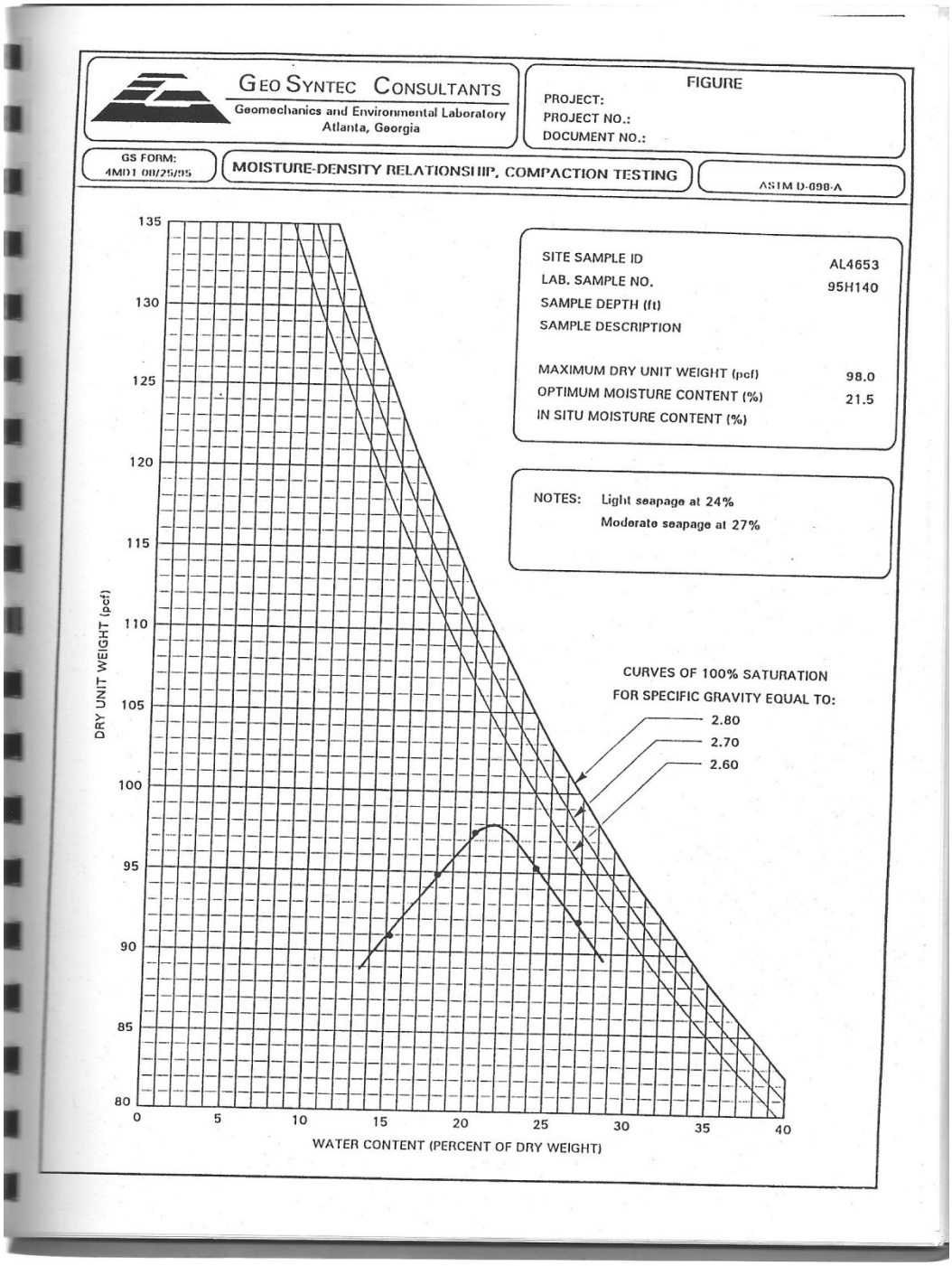

Figure B.12: Compaction report for Clay fill material.

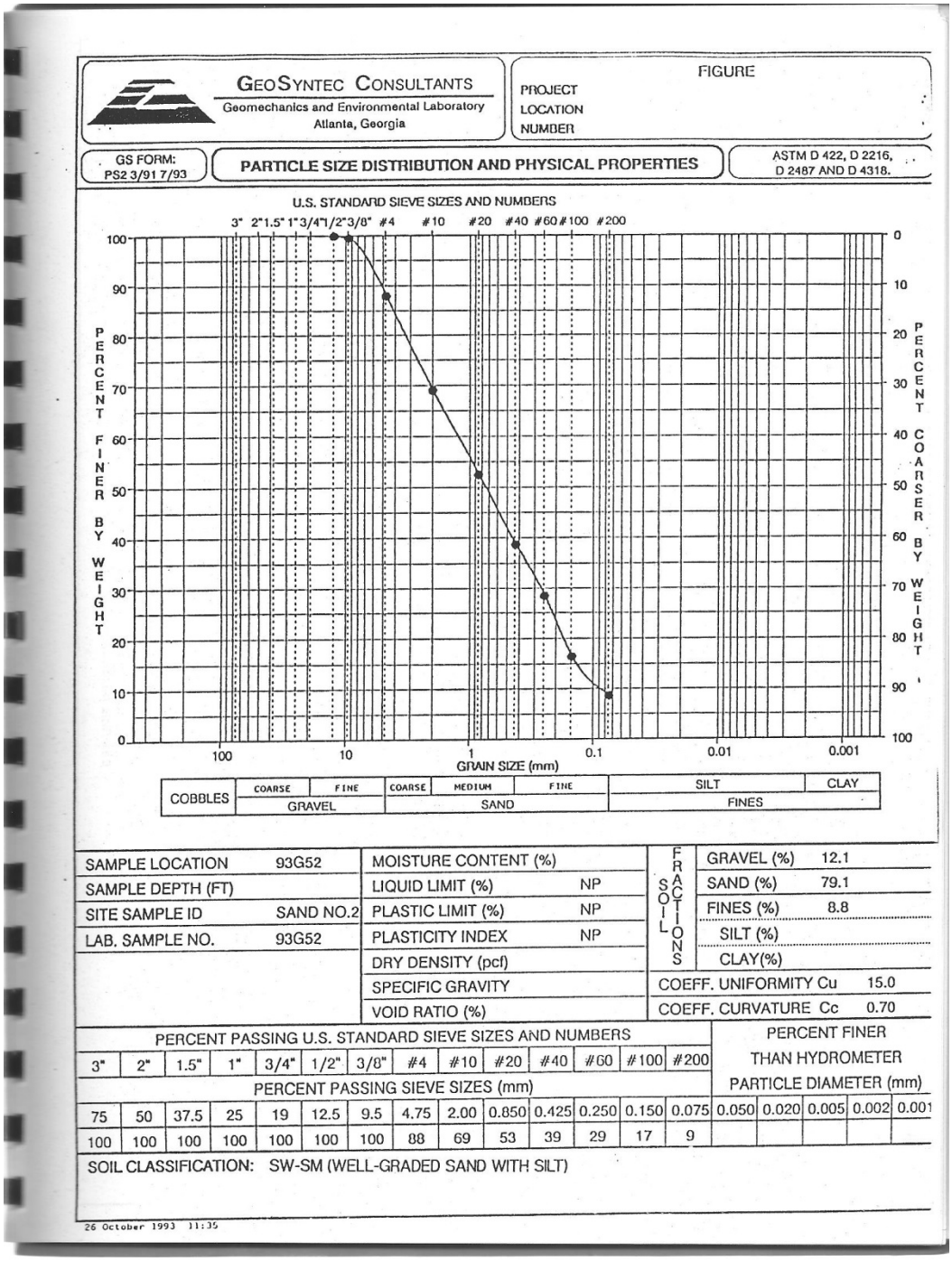

Figure B.13: Gradation report for Sand 7 fill material.

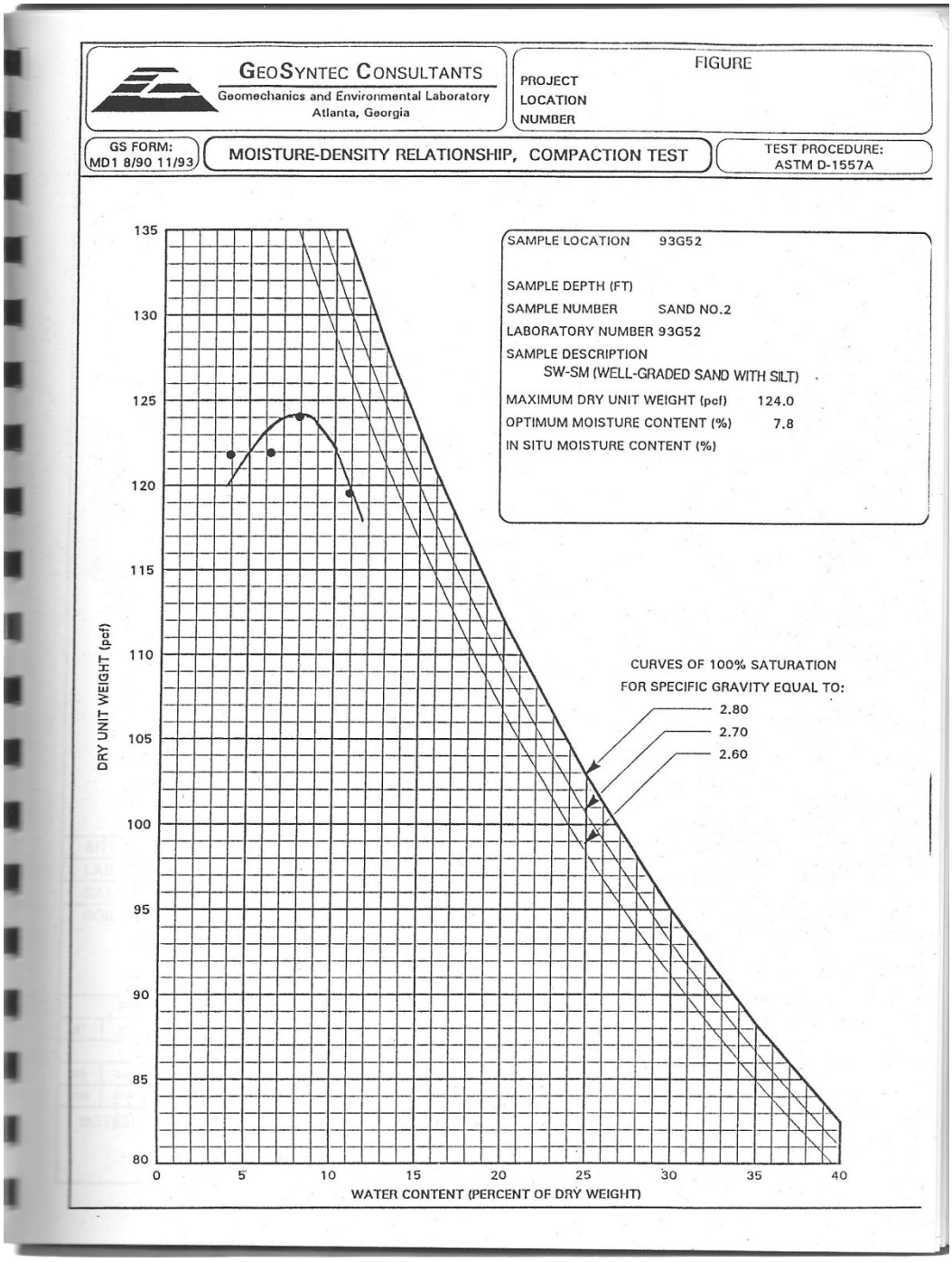

Figure B.14: Compaction report for Sand 7 fill material.

References

GeoSyntec Consultants 1992-2000. Soil Properties and Geogrid Pullout Testing. Multiple reports. GeoSyntec Consultants, Austin, TX

Koerner, R. M., Wilson-Fahmy, R. F. 1993. Finite element modeling of soil-geogrid interaction with application to the behavior of geogrids in a pullout loading condition.

Moraci, N., Recalcati, P. 2006. Factors affecting the pullout behavior of extruded geogrids embedded in a compacted granular soil. Geotextiles and Geomembranes.

Palmeira, E. M., Milligan, G. W. W. 1989. Scale and other factors affecting the results of pull-out tests of grids buried in sand. Geotechnique.

Teixeira, S. H. C. et al 2007. Pullout resistance of individual longitudinal and transverse geogrid ribs. ASCE Journal of Geotechnical and Geoenvironmental Engineering.